Summer 7-26-2020

The anti-diabetic potential of the African Adansonia Digitata L. plant extract

Marwa Tawfik Badawy
The American University in Cairo

The Anti-Diabetic potential of the African *Adansonia digitata* L. Plant Extract

A thesis submitted in partial fulfillment of
the requirements for the degree of
Master of Science in Biotechnology

By

Marwa Tawfik Badawy

B.Sc. Biotechnology

Under Supervision
Of

Prof. Dr. Ahmed Abdellatif
Assistant Professor
Biology Department

Prof. Dr. Mohamed A. Farag
Professor and Director of Food Chemistry
Program, Chemistry Department

School of Sciences and Engineering

Biotechnology Graduate Program
School of Sciences and Engineering
American University in Cairo

2020

Table of Contents

بسم الله الرحمن الرحيم

In the Name of Allah, the Most Gracious, the Most Merciful

Abstract

Diabetes Mellitus (DM) is a severe chronic disease affecting a large population worldwide. The Middle Eastern region has been gifted with lots of native medicinal plants. However, there is less information on development of these medicinal plants into nutraceuticals for modulating specific diseases such as diabetes of common occurrence regionally. Towards this end, there is a crucial need to investigate other types of treatments to modulate diabetes. This study is conducted to fill in this gap by investigating medicinal plant used as folk medicine, which is Baobab (*Adansonia digitata* L.). This study is performed in two phases: *in-vitro* and *in-vivo*. The *in-vitro* part included extraction, assessment, and characterization of the baobab fruit pulp crude extract. The cytotoxic activity was assessed using MTT assay on L-929 fibroblast cells, with an IC_{50} value of 105.7 µg/mL, whereas DPPH was used to assess the antioxidant activity with calculated IC_{50} at 114.8 µg/mL. To characterize metabolites mediating for these effects, ultrahigh performance (UHPLC) analysis coupled to MS revealed for a total of 77 metabolites belonging to different chemical classes including organic acids, sugars, alcohols, phenolics, coumarins, and fatty acids. Almost 50% of the identified metabolites are reported for the first time in *A. digitata* fruits. In the second phase, the extract was tested *in-vivo* in an experimental streptozotocin (STZ) induced Sprague Dawley male rat model of diabetes. *A. digitata L.* low dose (150 mg/kg) injected i.p. twice a week showed potential hypoglycemic activity as revealed from several biochemical parameters such as fasting blood glucose, alkaline phosphatase, and blood urea nitrogen levels in comparison to high dose (300 mg/kg). Overall, the current study proves that *Adansonia digitata* L. has good potential as an antidiabetic, hepatoprotective, and reno-protective drug with a good safety margin.

Keywords: Diabetes Mellitus, Middle Eastern plants, *Adansonia digitata* L., Diabetic animal model, metabolomics, metabolites, streptozotocin, STZ, Sprague Dawley rats

List of Figures

List of Tables

List of abbreviations

DM: Diabetes Mellitus

β-cells: Beta Cells

STZ: Streptozotocin

ALT: Alanine Amino Transferase

AST: Aspartate Transaminase

TG: Triglycerides

MTT: (3-[4,5-dimethylthiazol-2-yl]-2,5 diphenyl tetrazolium bromide)

DPPH: (2,2-diphenyl-1-picryl-hydrazyl-hydrate)

UPLC: Ultra Performance Liquid Chromatography

HPLC: High Pressure Liquid Chromatography

GC/MS: Gas Chromatography Mass Spectrometry

LC/MS: Liquid Chromatography Mass Spectrometry

UHPLC-MS: Ultrahigh-pressure (or performance) liquid chromatography – Mass Spectrometry

BPC: Base Peak Chromatogram

m/z: mass-to-charge ratio

DMEM: Dulbecco's Modified Eagle Medium

FBS: Fetal Bovine Serum

Pen-strep: Penicillin Streptomycin

MeOH: Methanol

DMSO: Dimethyl Sulfoxide

H&E: Hematoxylin & Eosin Stain

Dedication

To my beloved father and Mother

Any words will not be enough for your efforts with me since primary school. Thank you for always encouraging, supporting, and believing in me. Every single achievement in my life is because of you and will always be for both of you. ***Mr. Tawfik Badawy and Mrs. Eisha Abdel-Kreem****, I will always make you proud of me!*

To my twin sister, my brother, and my brother in law

My soulmate Maha Tawfik she is the second living part of me, and Mahmoud Tawfik the wised and supportive brother. Thank you both for always being by my side. My brother in law, my sister's Fiancé, Mahmoud Elfakhrany thanks a million for everything and for being by my side.

To my beloved friends

My best friends Manal Moustafa & Nehal Ibrahim thanks a trillion for always being my own shelter and great supporters. For my beloved friends, who helped me a lot Nahla Osama, Eman Khalil, Marina Nabil, Menna Nabil, Nehal Adel, and Yomna Adel.

Acknowledgment

I would like to express my sincere gratitude to my dearest professors who gave me unconditional help, support, and mentorship throughout my educational journey.

Dr. Ahmed Abdellatif, *our beloved thesis advisor, I would like to say thanks a zillion for always treating me like your daughter and acting as a second father for me. This work would not be done and be like this without your mentorship.*

Dr. Mohamed Farag, *I can't thank you enough for accepting me in your lab at Cairo University. I have learned a lot from you, and it's my honor to be in your team.*

Dr. Ahmed Moustafa, *thank you for being my mentor in the bioinformatics field and allowing me to be your TA. I really appreciate every single moment you guided and supported me.*

Dr. Samir Mohamed, *many thanks for your unlimited encouragement since I was in the genetics department in my bachelor's degree and your extended support during my master's degree as well.*

Dr. Mohamed Zakaria, *a great supporter during the bachelor's degree and the master's degree as well. Thank you for being by my side in every single moment I asked for your help.*

Last but not least, I would like to thank all of my colleagues at AUC and Faculty of Pharmacy, Cairo University, especially Dr. Mohamed Nabil. As well as, Dr. Ahmed Abdellatif's team, Dr. Alaa Fouad from Veterinary Medicine, and Dr. Nesrine Hegazy from National Research Center.

Chapter One: Introduction and Literature Review

1.1. Introduction:

Diabetes Mellitus (DM) is a chronic disease characterized by disturbed glucose metabolism, affecting an estimated 8.8 percent of the people worldwide, with an expected increase in this percentage to 9.9 percent in 2045. Egypt is among the top countries in the diabetic population in 2019 (Figure 1), with 8.9 million diabetic people (Elflein, 2019).

In 1550 BC, the Ebers papyrus contained a description of several diseases, including polyuric syndromes (Ebbell, 1937). Araetus (81-138 BC), another great scientist, also noted that diabetes is a sort of polyuric waste disorder (Araetus, 1856). The word "diabetes" means a urine fountain. Araetus stated that "Diabetes is a wonderful affliction being "melting" down of the flesh and limbs into urine" (Araetus, 1856). Furthermore, diabetes mellitus was well known for its association with "honey urine."

Diabetes (DM) has three major types, which are; type I, type II, and gestational diabetes (Colberg et al., 2016). Diabetes type I may be caused by autoimmune reactions destroying the pancreatic β-cells, resulting in a lack of insulin. Therefore, type I is insulin-dependent, and patients rely on the external supply of insulin for life. On the other hand, diabetes type II, the most common type, is non-insulin-dependent. Gestational diabetes occurs during pregnancy; however, the mothers could develop type II DM later on (Dyck, 2003). Pre-diabetes is a term commonly used to describe conditions where blood glucose level is higher than the normal, but not high enough for DM diagnosis (figure 2) to be made (Prevention, 2020). Some risk factors are associated with diabetes, such as obesity, hypertension, and hyperlipidemia (Steyn & Damasceno, 2006).

To date, there is no cure for diabetes (Prevention, 2020). The management of DM is not without disadvantages and complications such as drug resistance and toxicity. Additionally, uncontrolled diabetes could result in chronic complications such as blindness, heart disease, and renal failure (Mamun-or-Rashid et al., 2014). Hence, there is a crucial need to investigate other types of treatment to modulate this chronic disease.

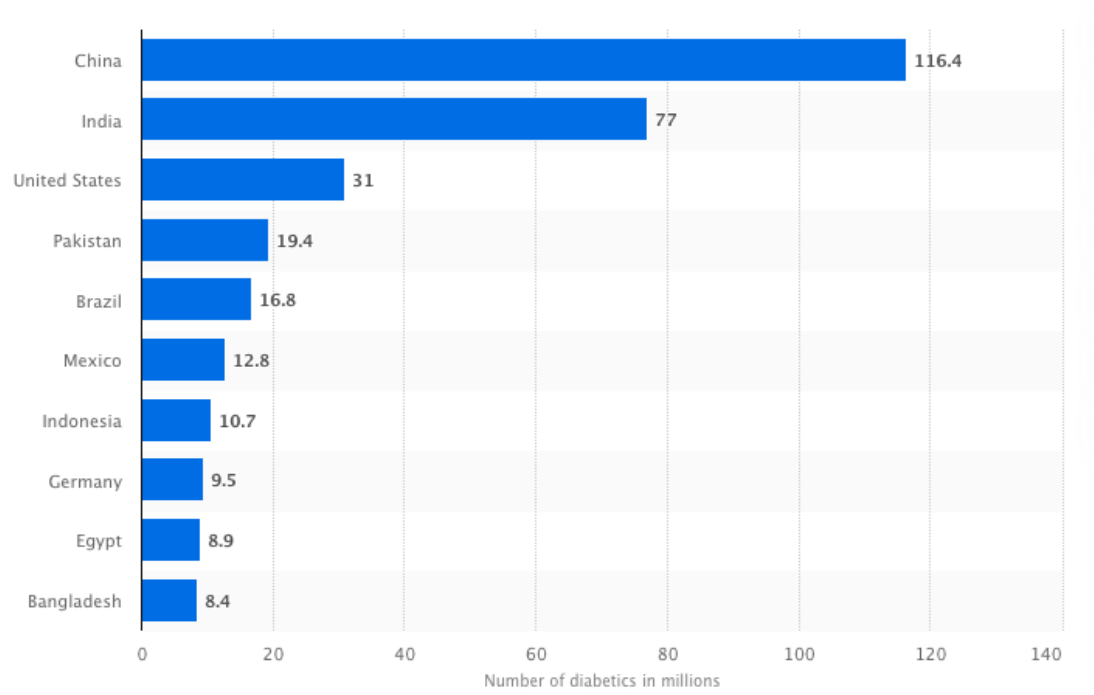

Figure 1: Estimated number of diabetic population worldwide in 2019**,** *(Elflein, 2019).*

The Middle East region is rich with medicinal plants used as folk medicines that have a great impact on diseases like DM (Özturk, Altundag, & Gucel, 1999). However, their side effects must be considered before use (P. Gupta, 2012; Kooti, Farokhipour, Asadzadeh, Ashtary-Larky, & Asadi-Samani, 2016; Mamun-or-Rashid et al., 2014). Although there is an abundance of literature worldwide on the use of plant extracts in diabetes, there are few reliable studies on Baobab (Tabaldi) "*Adansonia digitata L.,"* a plant native to Africa and traditionally used to treat DM.

Therefore, the aim of the current study is to investigate this crude plant extract and characterize its effects on diabetic complications in a well established experimental animal model of diabetes (Srinivasan & Ramarao, 2007). Animal models may be considered cruel by animal rights activists. We believe that such models, when humanely and appropriately used, provide an excellent opportunity to study diseases and provide significant pre-clinical studies that would improve patient care worldwide. (Rees & Alcolado, 2005).

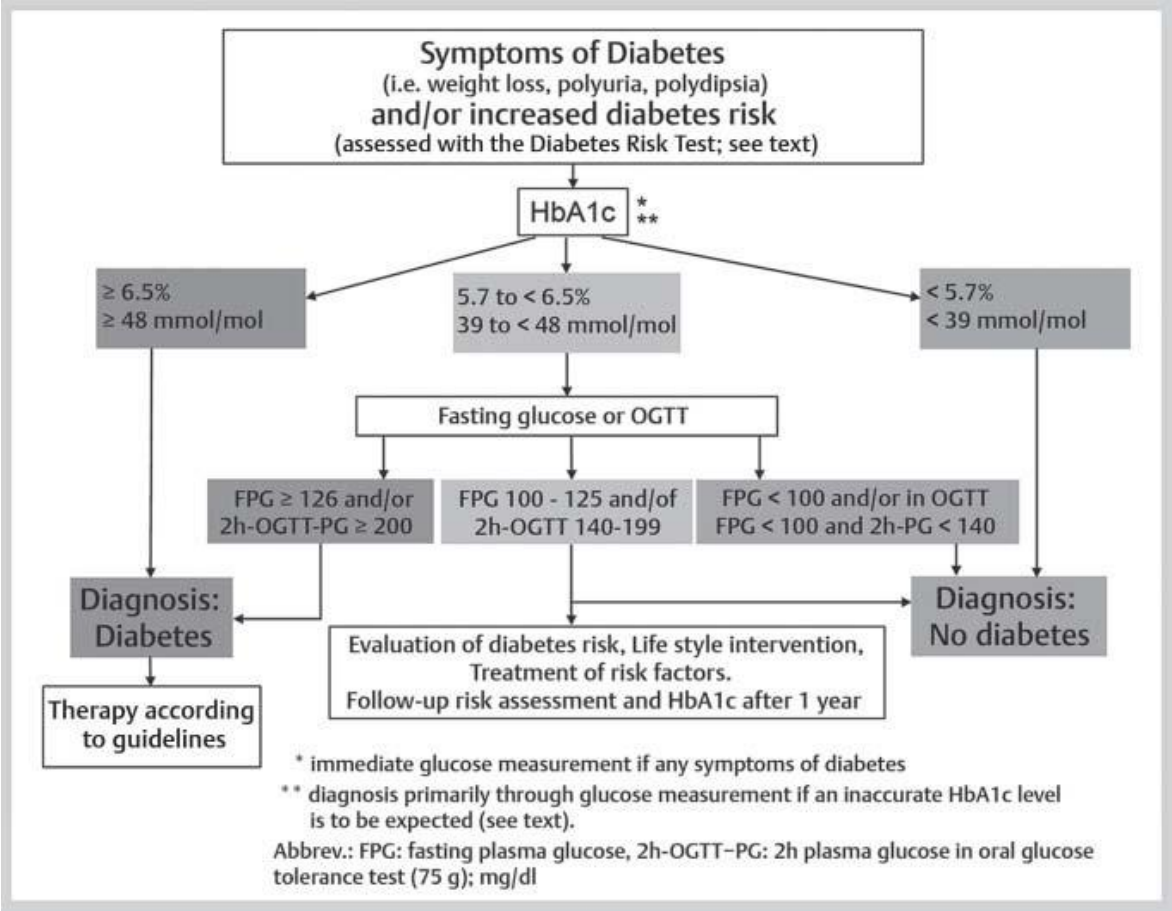

Figure 2: *Diabetes Mellitus* Diagnostic flowchart *(Kerner & Brückel, 2014)***.**

1.2 Hypothesis

The *Adansonia digitata L.* fruit pulp crude extract will have beneficial antidiabetic effects in STZ-diabetic rats.

Aims:

- Extraction and characterization of *Adansonia digitata* L. plant.
- *In vitro* testing of the cytotoxic and antioxidant activities of the plant extract.
- *In vivo* testing of the plant extract, in an animal model of *Diabetes Mellitus*.

1.3 Animal Models of Diabetes

Experimental animal models of diabetes mellitus (DM) can be divided into three main groups; chemical, surgical, or genetically-induced diabetes (S. Kumar, Singh, Vasudeva, & Sharma, 2012). Chemical induction of diabetes is achieved with diabetogenic agents, such as Streptozotocin (STZ), Alloxan (ALX), Goldthioglucose (GTG), as well as other drugs such as antipsychotic drugs. These chemicals either cause entire damage of the ß- cell, develop an inhibition of insulin production and secretion, and decrease or minimize the metabolic productivity of insulin in the targeted tissues (M. P. Singh & Pathak, 2015). The most commonly used chemicals for diabetes mellitus induction in animals are Streptozotocin (STZ) and Alloxan (ALX), which are usually injected either intraperitoneal (IP), subcutaneous (SC), or intravenous (IV) injections.

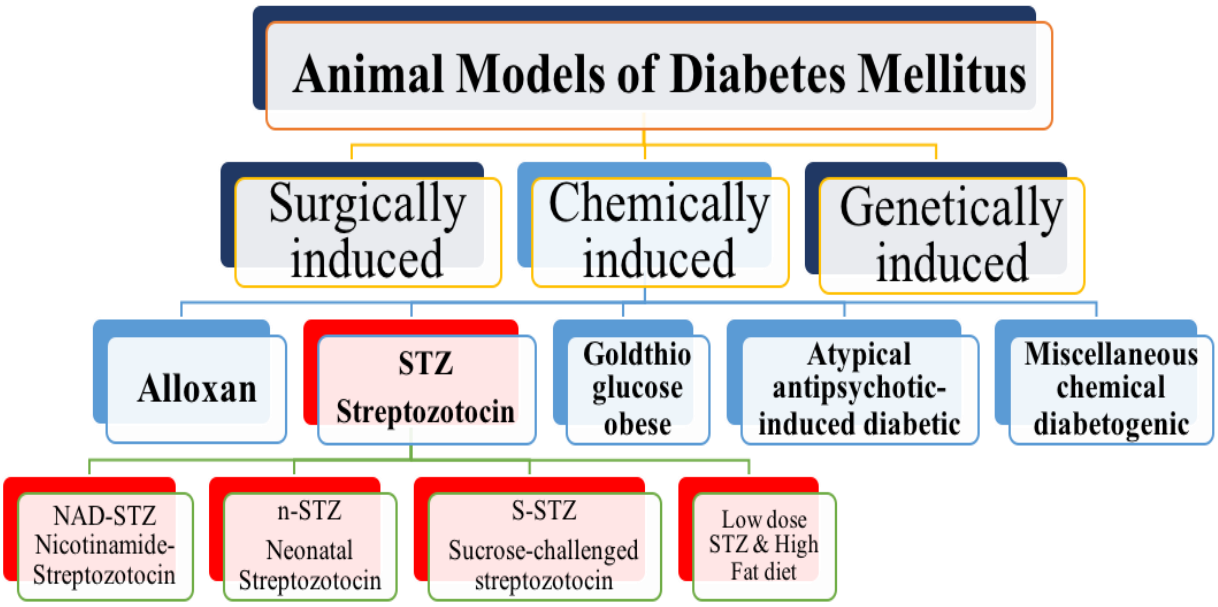

Figure 3: Schematic flow chart of the induced animal models of *diabetes mellitus*.

The second type of diabetic model is surgically induced by either partial (to induce type II DM) or complete removal of the pancreas to induce type I DM (Ozturk, Atlan, & Yildizoglu-Ari, 1996).

However, pancreatectomy is not widely accepted nowadays by researchers for diabetic investigations (Rees & Alcolado, 2005).

The third type is genetically induced diabetes in animals, using several mutations such as (db/db mice), or induction from non-diabetic outbred animals by the repeated breeding. The general concept behind the mutation induction in animals is that a single or multigene defect cause diabetes. Other genetically induced diabetic models are Zucker diabetic fatty rat, Goto-Kakizaki rat, LEW.1WR1 rats, NONcNZO10 mouse, C57BL/6J mice, Kuo Kundo mice, Tsumara Suzuki Obese Diabetes mice, db/db mice, and Obese rhesus monkey (Macaca mullata) (Ktorza et al., 1997).

There are also other unclassified models of diabetes, such as virus-induced diabetic animal model, Oral glucose loading animal model, Insulin Antibodies-induced diabetes, and In-vitro models for diabetes (Ktorza et al., 1997).

1.4 Streptozotocin-Induced Diabetic Model

Streptozotocin (STZ) is a glucosamine-nitrosourea complex initially marketed under the name of Zanosar® (R. B. Weiss, 1982). It is the most commonly used diabetogenic drug in inducing diabetes to all species (Junod, Lambert, Stauffacher, & Renold, 1969). Rats, mice, hamsters, dogs, monkeys, and sheep STZ-induced models of diabetes using a wide range of doses in single or multiple injections have been reported widely in the literature (P. Kumar, Kale, & Baquer, 2012; Srinivasan & Ramarao, 2007). In large animals, STZ can be combined with partial pancreatectomy to develop diabetes.

Streptozocin (STZ) is a selective cytotoxic agent that specifically destroys pancreatic β cells. Streptozotocin enters the pancreatic β cells through the glucose transporter 2 (GLUT2). Since STZ consists of two parts, which are glucose and methyl nitrosourea, it splits, and the methyl nitrosourea moiety acts as an alkylating agent, causing DNA alkylation and will destroy the cells (Szkudelski, 2001). However, the cells producing insulin in the pancreas could have some resistance from STZ if they do not have GLUT2 (Ledoux & Wilson, 1984).

There are several modifications of the STZ induced model, e.g., Neonatal STZ induced diabetes rat model (n-STZ), Nicotinamide-Streptozotocin (NAD-STZ) induced model, Sucrose-challenged STZ-induced rat model (STZ-S), and the Low dose STZ with high-fat diet rat model (M. P. Singh & Pathak, 2015). The low dose STZ / high-fat diet rat model is the closest to DM type II in humans and is commonly used for pharmacological screening (Srinivasan, Viswanad, Asrat, Kaul, & Ramarao, 2005).

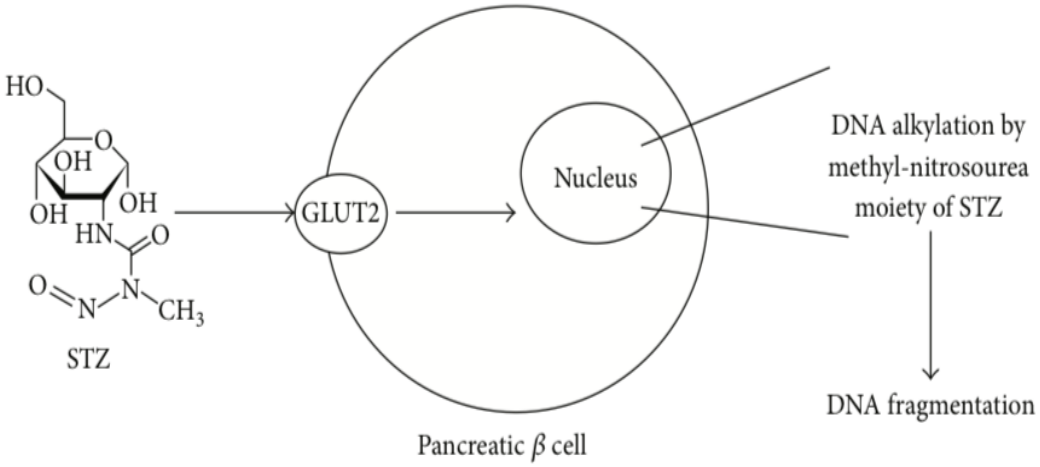

Figure 4: Mechanism of action of streptozotocin (STZ).

STZ enters the β-cells by the GLUT2 receptor (Glucose Transporter 2), causing DNA fragmentation and cell death (Al-Awar et al., 2016).

1.5 Commonly used anti-diabetic medicinal plants

Commonly used medicinal plants in folk medicine, as anti-diabetic plants, are available in the Middle Eastern region such as Tabaldi, (Baobab) (*Adansonia digitata L.*), Kaff Maryam (*Anastatica hierochuntica L.*), Argel (*Solenostemma Argel*), Fenugreek (*Trigonella foenum-graecum*), Hanzel (*Citrullus colocynthis*), Curcumin (*Turmeric*), Cinnamon (*Cinnamomum Zeylanicum*), and Mango (*Mangifera indica*). In this study, we will focus on Baobab (*Adansonia digitata L.*) plant extract, which is native to Sudan and is commonly used in folk medicine as an anti-diabetic treatment.

Fenugreek has some antibacterial, gastric stimulant, anti-diabetic, anticancer, and hepato-protective effects (Srinivasan, 2006). Caffeic acid & Ellagic acid have some effects in decreasing the plasma glucose levels in diabetic model mice, which are present in fenugreek (Chao, Hsu, & Yin, 2009). The methanolic extract of Argel, it has antioxidant and hypoglycemic effects without any reported toxicity. However, there is little research conducted to investigate its mechanism of action (Deen & Al-Naqeb, 2014). Kaff Maryam methanolic extract significantly increased IgG levels after a dose of 50 mg/kg, which was believed to have some effects on β-cell function (Abdulfattah, 2013).

In a clinical trial, 125 mg per day of Hanzel for 2 months showed an increase in HbA1c and Fasting BS with patients diagnosed with type II diabetes without any side effects reported (Barghamdi et al., 2016). In another clinical trial using Curcumin, lowering of triglycerides, alanine aminotransferase (ALT), and beta-amyloid was seen (S. C. Gupta, Patchva, & Aggarwal, 2013).

Cinnamon showed a very good ability to normalize glucose metabolism, weight changes, and lipid abnormalities in an STZ animal model of diabetes (Anand, Murali, Tandon, Murthy, & Chandra, 2010). Mango can decrease hyperglycemia in diabetic rats at concentrations of 5, 10, and 15% (Perpetuo & Salgado, 2003). Phytochemical analyses were performed for the methanolic mango extract, and it showed the presence of glycosides, flavonoids, tannins, saponins, terpenoids, and steroids (Gwarzo & Bako, 2013; Zekry, Badawy, Ezzelarab, & Abdellatif, 2020).

There are currently few reliable studies of the *Adansonia digitata* L. effects on diabetes and its complications such as (Bako, Mohammad, Waziri, Bulus, & Zubairu., 2014) . As a result, this study is designed to provide a further investigation of its effects as well as its mode of action.

1.6 Origin and history of the *Adansonia* genus

The tree of *Adansonia* genus occurs mainly in Africa, especially in Madagascar, and in Australia (Baum, 1995). It was named *Adansonia* after the frensch botanist Micheal Adanson who discovered it in Senegel in 1749. It is also known as the upside-down Baobab tree or monkey bread tree. The name is based on the Arabic word *bu hobab*, meaning “fruit with multiple seeds.” There

are eight different species of Baobab, including six that are native to Madagascar, one to Australia, and another one to the African mainland (Baum, Small, & Wendel, 1998). The Baobab tree has diverse uses by the African people (Baum, 1995).

The first species is *Adansonia digitata* L. *(Malvaceae)* or African baobab, which is distributed across the African continent. *Adansonia digitata s.l.* is another one consisting of the diploid *A. kilima* and the tetraploid *A. digitata s.s.* (Pettigrew et al., 2018). The *A. digitata s.s.* is distributed across the African Sub-Sahara extending from the northern Sahel to South Africa. However, it is not likely to be present in the center of Africa, especially in the rainforest areas, as well as the high elevation above 800 meters of the eastern African area (Gerald E. Wickens & Lowe, 2008).

The phylogeographic analyses showed that the *Adansonia digitata s.l.* Populations are native to eastern and western Africa. Moreover, they are genetically distinct from these particular areas (Pock et al., 2009). The *A. digitata* and *A. kilima* show high genetic similarity. These analyses also indicate that the evolution of the tetraploid species is occurring recently (Pettigrew et al., 2018; Gerald E. Wickens & Lowe, 2008).

Baobabs are known for their high nutritional value as a cultural fruit. The fruit is consisting of seeds surrounded by the powdery pulp in a hard endocarp. The fruit taste is sweet and sour, which is liked by many people who consume it on a regular basis. However, the seeds are not edible until they are roasted or ground (Gebauer, El-Siddig, & Ebert, 2002). People used to consume it by discarding the seeds or allowing them to pass as they are in the digestive system after eating the fruit pulp. Furthermore, some genetic analyses are suggesting that the spread and distribution of the baobab tree over the continent of Africa is due to human practices (Pock et al., 2009).

The African baobab species spread to other regions located around the Indian Ocean, such as Yemen, Comoros, and southern Iran (Parsa, 1959). The immersion of the baobab fruit in seawater showed tolerance and no effect on the viability of the fruit itself even after six months of immersion in that salt condition (Pock et al., 2009). This might provide an explanation of the presence of the baobabs in the coastal regions across the Indian subcontinent (Gerald E. Wickens & Lowe, 2008).

Some specific populations sharing the same genetic ancestors of baobabs were grouped in the Mascarene Islands, southeast India, Malaysia, and West Africa because of the German, French,

and English people and their movements between the Asian and African continents (Burton-Page, 1968).

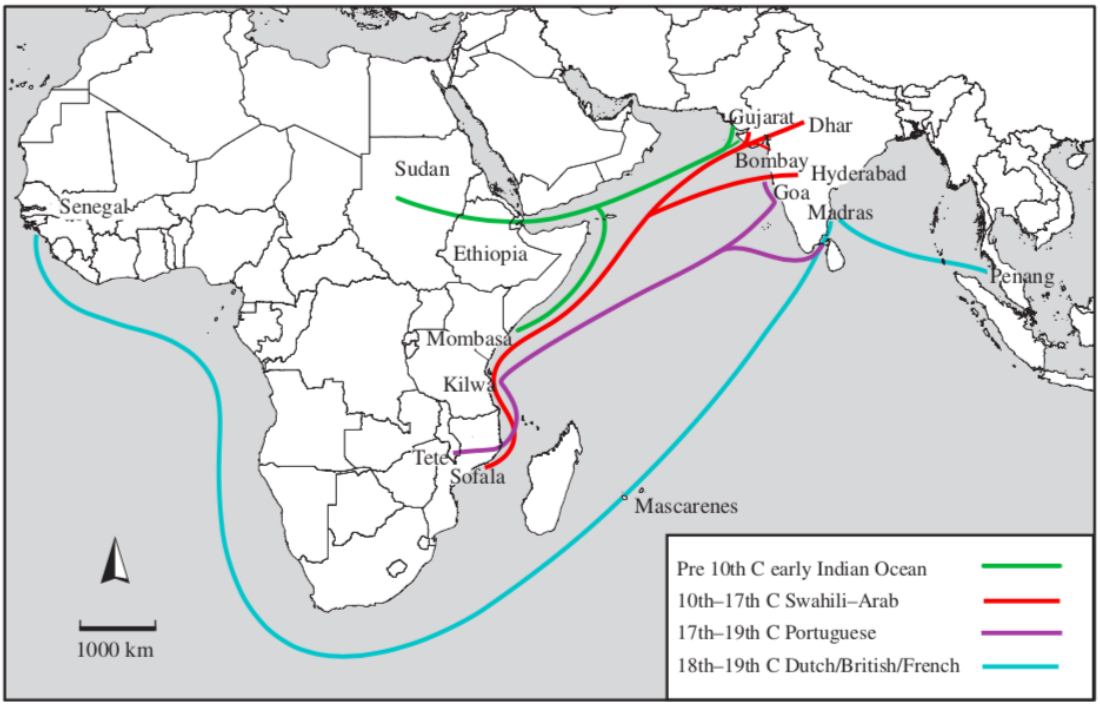

Figure 5: The spread of the *Adansonia digitata* L. tree from Africa.

The introduction of the Baobab species from Africa to the Indian subcontinent. Due to the trade through the ocean during various periods (Bell, Rangan, Kull, & Murphy, 2015).

1.7 *Adansonia digitata L.* plant in Folk Medicine

Tabaldi, Baobab., is called "The small Pharmacy" because of its huge contribution to folk medicine (Obizoba & Anyika, 1994). The fruit pulp is very rich in nutrients as well as carbohydrates, calcium, potassium, thiamine, nicotinic acid, and vitamin C (G. E. Wickens, Goodin, & Field, 1985). Phytochemical analyses for the methanolic extract showed the presence of glycosides, flavonoids, tannins, saponins, terpenoids, and steroids. In addition, this methanolic extract from

the fruit pulp showed anti-diabetic effects in Alloxan induced diabetes models (Gwarzo & Bako, 2013).

All parts of the baobab are edible, e.g., seeds, roots, flowers, leaves, bark, and fruit pulp. The trees of Baobab can be grown even in high temperatures and be resistant to it for a long period of time. Baobabs are known for their excellent antioxidant and anti-inflammatory properties since ancient times. It is also used to treat several microbial infections as traditional medicine. Soups can be prepared from the baobab leaves, and these soups can be thickened by the addition of the seeds. Furthermore, the seeds can be roasted in order to be used as snacks (Caluwé, Halamová, & Damme, 2010). Baobab fruit includes pulp with large seeds embedded in the acidic pulp. The pulp is used for food recipes as well as making some beverages (Obizoba & Anyika, 1994).

The bark, leaves, and fruits of *Adansonia digitata* are used as medicinal plants in South Africa. Fresh bark beverage is used for cold and influenza symptoms (Sulaiman et al., 2011). Furthermore, the seeds, wood, and bark of the baobab are used as anti-inflammatory agents (Selvarani & James, 2009). The leaves are famous for treating fevers, kidney, and bladder diseases. In addition to their effects on asthma and diarrhea. A mixture of the flour of pulp mixed with millet flour and water is given to the children for the treatment of the infant diarrhea (Lockett, Calvert, & Grivetti, 2000). *Adansonia digitata* L. plant showed potential antiviral effect against three tested viruses including herpes simplex, polio, and Sindbis (Ananil, Hudson, & Souzal, 2000).

In West Africa, the seeds, fruit pulp, and the leaves are considered as essential components in sauce preparation (Caluwé et al., 2010). Baobabs are also called “super fruit” thanks to their high nutrition value of vitamins, minerals, and fatty acids contents (Gruenwald, 2009). The baobab products are important because of their dietary fibers and ascorbic acid components. The fruit is considered as one of the richest fruits in Vitamin C, which is present in a range of 2.8 to 3 g/kg in the fruits (Silvia Vertuani, Braccioli, Buzzoni, & Manfredini, 2002). Another study revealed that the percentage of vitamin C present in the fruit pulp is (280-300 mg/100 g), which is seven times the vitamin C content found in the oranges (51 mg/100 g) (Manfredini, Vertuani, & Buzzoni, 2002). A recent study stated that the baobab pulp could provide 100% of the recommended daily intake of vitamin C for pregnant females when consuming 40 g of the fruit (Chadare, Linnemann,

Hounhouigan, Nout, & Van Boekel, 2008). Regarding the actual content of the ascorbic acid, it was found that the fruit pulp contains 337 mg/100 g (Eromosele, Eromosele, & Kuzhkuzha, 1991).

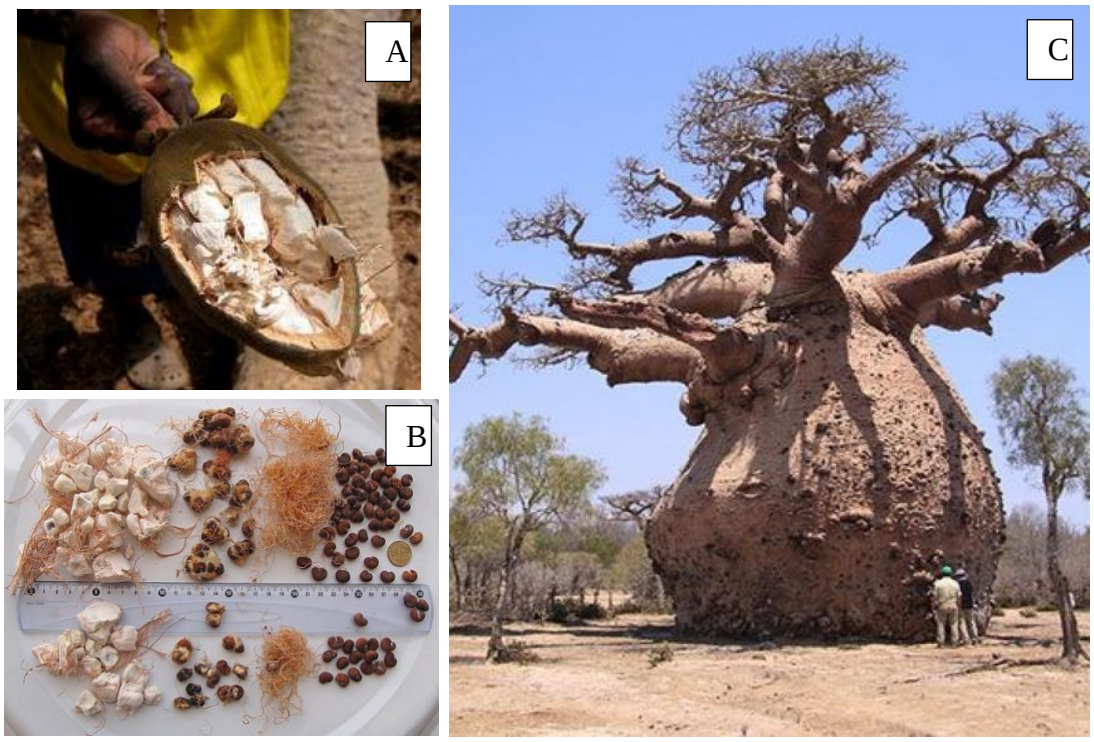

Figure 6: *Adansonia digitata* L. Plant

(A): The Baobab fruit pulp. **(B**)The Baobab fruit pulp and seeds. **(C)** The upside-down Baobab tree picture. Source: wo.wikipedia.org.

1.8 Chemical content of *Adansonia digitata L.*

The seed of the *Adansonia digitata* L. contains high amounts of fat (12.2 ± 0.2%), crude fiber (16.3 ± 9.3%), and protein (18.4 ± 0.5%). The *Adansonia digitata L.* seed oil is a great source of mono as well as polyunsaturated fatty acids. The composition of the oil is mostly saturated fatty acids, monounsaturated fatty acids, and polyunsaturated fatty acids at 31.7%, 37%, and 31.7% respectively. The oleic acid is the major fatty acid with 35.8%, then the linoleic 30.7%, and finally the palmitic 24.2% (Lockett et al., 2000; Ralaimanerivo, Gaydou, & Bianchini, 1982).

The fruit pulp is considered a great source of carbohydrates (76.2 ± 1.0%), low fat (0.3 ± 0.0%), and low protein (8.2 ± 0.1%). The fruit pulp and seed are great sources of calcium, magnesium, and potassium.

Amino acids content in both seed and fruit are presented by high amounts of aspartic acid, arginine, and glutamic acid (Glew et al., 1997).

The leaf extract contains succinic, lactic, malic, citric, formic, and fumaric acids were identified as well as the fruit pulp. The RP-HPLC-PDA-ESI-MS/MS (High Performance Liquid Chromatography-Photo Diode Array-Electrospray Ionization-Mass Spectrometry) analysis also confirmed some organic acids including citric acid at 77.3%, malic acid (17.6%), ascorbic acid (3.2%), and gallic acid (1.3%) (Tsetegho Sokeng et al., 2019).

Phenolic analysis revealed variety of classes such as tannins, flavones, and flavonols. Flavonoids (flavanols, flavones, flavonols, and proanthocyanidins) as well as the non-flavonoids (hydro-xycinnamic derivatives) were detected in the baobab fruit pulp (Tsetegho Sokeng et al., 2019). Furthermore, hydroxy cinnamates were identified by (N. X. Li et al., 2017) and proanthocyanidins by (Shahat, 2006).

Table 1: Summary of the previously reported work on the anti-diabetic and chemical composition of the *Adansonia digitata* L.

Plant Part	Type of extraction	Route of administration	Chemical composition	Chromatographic analysis - Fractionation	Reference
Fruit pulp	Methanol and Millipore grade water acidified with formic acid (0.1%)	N/A	- Sugars and derivatives - Organic acids - Amino acids - Phenolic compounds	RPHPLC-PDA-ESI-MS/MS	(Tsetegho Sokeng et al., 2019)
	Ethyl Acetate	N/A	- hydroxycinnamic acid glycosides (HAGs) - iridoid glycosides (IGs) - phenylethanoid glycosides (PGs)	UHPLC-DAD-HRMS	(N. X. Li et al., 2017)
	Ethyl Acetae	N/A	- proanthocyanidin	TLC	(Shahat, 2006)
	Methanol	Intraperitoneally/ Orally	N/A	N/A	(Bako et al., 2014)
	Aqueous	Orally	N/A	N/A	(Muhammad, Jarumi, Alhassan, Wudil, & Dangambo, 2016)
Leaves	Methanol and Millipore grade water acidified with formic acid (0.1%)	N/A	- Sugar and derivatives - Organic acids - Amino acids - Phenolic compounds	RP-HPLC-PDA-ESI-MS/MS	(Tsetegho Sokeng et al., 2019)

Chapter two: Materials and Methods

2.1. Extract preparations

Adansonia digitata L. was purchased from the local market in Sudan. The fruit pulp was crushed and ground into powder. Alpha Chemika Methanol reagent M.W.= 32.04 was used in preparing the crude extract. This powder was dissolved in methanol at a ratio of 2:10, 100 grams were soaked in 500 ml methanol for 48 hours. The extract was filtered using Whatman filter paper No. 1. The rotary evaporator Rotavapor® BÜCHI was used to evaporate the methanol from the extract, and the sample was left to air dry for 3-5 days in a hood. The extract was prepared freshly for further use (modified from (Bako et al., 2014)).

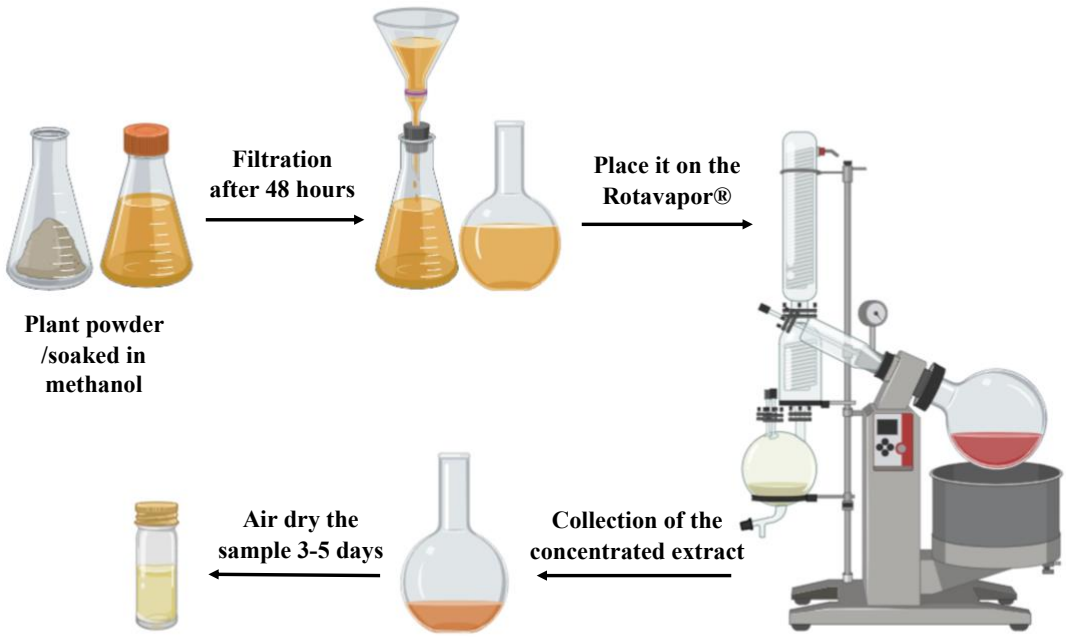

***Figure 7**: Adansonia digitata* L. plant crude extract preparation procedure

2.2. Cytotoxicity Assay (MTT)

3-[4,5-dimethylthiazol-2-yl]-2,5 diphenyl tetrazolium bromide assay was used to measure the cell viability. Cell's mitochondrial activity can be indicated by the conversion of the tetrazolium salt MTT into formazan crystals. The viable cell number is measured by detecting the formazan optical density (OD) at 570 to 720 nm. The MTT assay is widely used for the measurements of the drug sensitivity in cell lines and primary cells (van Meerloo, Kaspers, & Cloos, 2011).

L929 fibroblast cells (ATCC® CCL-1™, 100 old-day male rat) were seeded in 96-well plates in Dulbecco's Modified Eagle Medium (DMEM) supplemented with 1% Penicillin-Streptomycin antibiotic and 5% Fetal Bovine Serum (Canfield, 2010). The cells were incubated for 24 hours in Thermo Scientific™ Heracell™ VIOS CO2 incubator with 37° C and 5% CO_2. The media was removed, and the control, blank, and extract were added to the cells. After the second incubation of 24 hours, the media was removed, and the MTT (3-[4,5-dimethylthiazol-2-yl]-2,5 diphenyl tetrazolium bromide) reagent was added and incubated for 4 hours. Finally, the MTT was removed, and Dimethyl sulfoxide (DMSO) was added to the wells. The optical density (OD) was measured using SPECTROstar® Nano plate reader at 570 nm (modified from (van Meerloo et al., 2011)).

2.3. Antioxidant Activity Using (DPPH)

DPPH is the abbreviated term of free radical α, which is 2,2-diphenyl-1-picryl-hydrazyl-hydrate (DPPH; C18H12N5O6, M=394.33). This assay aims at the determination of the antioxidant activity by the use of the stable free radical of α. DPPH depending on the scavenging capacity measurement of the antioxidant agents (Blois, 1958). It works by the odd electron of the DPPH nitrogen atom is being reduced by receiving the hydrogen atom from the tested antioxidant material (Contrerasguzman & Strong, 1982).

The DPPH powder is prepared by weighing 3.94 mg and dissolving it in 100 ml methanol or ethanol for 0.1 mM solution preparation. This assay was performed in a 96-well plate. In brief, 50 µL of the DPPH solution are added to 150 µL of the tested extract (ratio of 1 ml DPPH to 3 ml of the tested sample). The mixture is allowed to stand in the dark with vigorous shaking at room

temperature for 30 minutes. Finally, the absorbance of the different concentrations was obtained using a SPECTROstar® Nano plate reader at 517 nm optical density. Ascorbic acid was used as a strong antioxidant material (modified from (Chiabchalard, 2013)).

2.4. (UHPLC/MS-MS) Analysis

2.4.1. Preparation of fruit extracts for UHPLC-MS analysis

Briefly, the freeze-dried fruits were ground with a pestle in a mortar, then 2 g of each fruit powder was homogenized with 5 mL 100% MeOH containing 10 µg/mL umbelliferone (an internal standard used for relative quantification of UHPLC-MS features) (Guillarme & Veuthey, 2017). Extracts were then vortexed vigorously and centrifuged at 3000 g for 30 min to remove plant debris. For solid-phase extraction, 500 µL were aliquoted and loaded on a (500 mg) C18 cartridge, which was preconditioned with methanol and water. Samples were then eluted with 3 mL 70% MeOH and 3 mL 100% MeOH. The eluents were evaporated to dryness under a gentle nitrogen stream. The obtained dry residue was re-suspended in 500 µL methanol for further UHPLC-MS analysis (modified from (Guillarme & Veuthey, 2017)).

2.4.2. High-resolution UHPLC-MS analysis

The UHPLC analysis was performed on an Acquity UHPLC System (Waters) equipped with a HSS T3 column (100 × 1.0 mm, particle size 1.8 µm; Waters). The analysis was carried out by applying the following binary gradient at a flow rate of 150 µL min−1: 0–1 min, isocratic 95% A (water/formic acid, 99.9/0.1 [v/v]), 5% B (acetonitrile/formic acid, 99.9/0.1 [v/v]); 1–16 min, linear from 5 to 95% B; 16–18 min, isocratic 95% B; and 18–20 min, isocratic 5% B (M. Farag, Mahrous, Lübken, Porzel, & Wessjohann, 2013).

The injection volume was 3.1 µL (full loop injection). Eluted compounds were detected from m/z 90 to 1000 using a MicroTOF-Q hybrid quadrupole time-of-flight mass spectrometer (Bruker Daltonics) equipped with an Apollo-II electrospray ion source in negative and positive (deviating values in brackets) ion modes using the following instrument settings: nebulizer gas, nitrogen, 1.4 (1.6 bar); dry gas, nitrogen, 6.l min−1, 190 °C; capillary, −5000 V (+4000 V); endplate offset, 500

V; funnel 1 RF, 200 Vpp; funnel 2 RF, 200 Vpp; in-source CID energy, 0 V; hexapole RF, 100 Vpp; quadrupole ion energy, 5 eV (3 eV); collision gas, argon; collision energy, 7 eV (3 eV); collision RF, stepping 150/350 Vpp (200/300 Vpp), (timing 50/50); transfer time, 58.3 μs; prepulse storage, 5 μs; pulser frequency, 10 kHz; and spectra rate, 3 Hz. Internal mass calibration of each analysis was performed by infusion of 20 μL 10 mM lithium formate in isopropanol[thin space (1/6-em)]:[thin space (1/6-em)]water, 1[thin space (1/6-em)]:[thin space (1/6-em)]1 (v/v), at a gradient time of 18 min using a diverter valve. For Auto-MS/MS analysis, precursor ions were selected in Q1 with an isolation width of ±3–10 Da and fragmented at collision energies of 15–70 eV using argon as collision gas. Product ions detection was performed using the same settings as above, but with funnel 2 RF 300 Vpp in negative mode (Mohamed A. Farag et al., 2016).

2.5. Animals and Induction of Diabetes

All experiments were conducted in accordance with the NIH guidelines for Animal Care and Use. Animal use protocol was approved by MSA University, Faculty of Biotechnology Animal Care and Use Committee (Courtesy of Dr. Mona Saadeldin, MSA University). Male Sprague Dawley rats weighing 150 - 200 g were maintained in a temperature-controlled environment at approx. 24 °C with a 12-h light/dark cycle and ad libitum access to food and water.

Streptozotocin (STZ) was injected intraperitoneally at a dose of 65-75 mg/kg (Furman, 2015) (Bonnevie-Nielsen, Steffes, & Lernmark, 1981; Srinivasan & Ramarao, 2007). Confirmation of diabetes was performed by measuring blood glucose levels using samples collected from the tail vein 3-5 days after the injection. Animals with glucose concentration > 250 mg/dL were considered diabetic and included in further experimentation. Pancreatic tissue histological examination after animal termination confirmed Diabetes mellitus (Qinna & Badwan, 2015).

The rats were randomized into six groups (Altman, 2002); each group consisted of 6 rats. The groups were:

1st group: normal control healthy (negative control),

2nd group: diabetic control untreated (positive control),

3rd group: diabetic + metformin (administered orally in the drinking water),

4th group: normal healthy + High dose (300 mg/kg) of *adansoina digitata* L. extract (intraperitoneally, twice a week),

5th group: diabetic + low dose (150 mg/kg) of *adansoina digitata* L. extract (intraperitoneally, twice a week),

6th group: diabetic + high dose (300 mg/kg) of *adansoina digitata* L. extract (intraperitoneally, twice a week) (modified from (Bako et al., 2014)).

The study duration was 4 weeks. Blood glucose and body weight were monitored twice a week. After four weeks, the rats were sacrificed, and blood and tissue samples were collected for biochemical (renal function, liver function, and lipid profile) and histological testing.

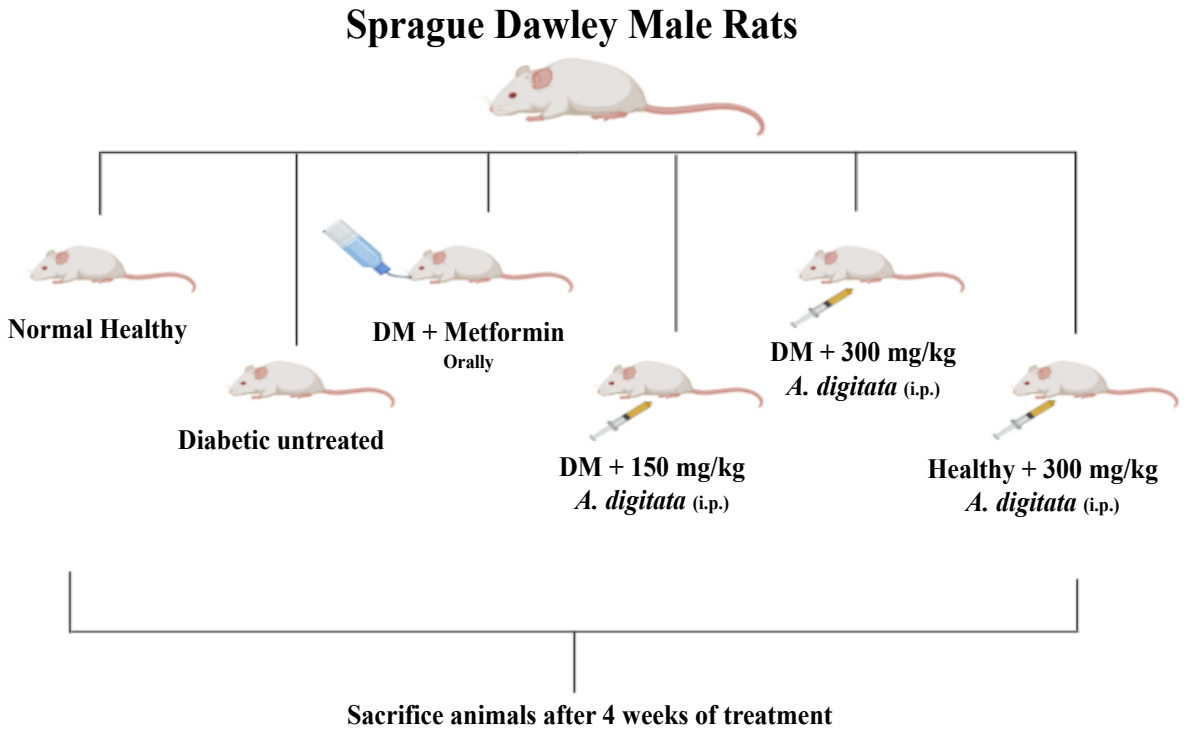

Figure 8: Sprague Dawley Male Rats' groups flow chart

2.6. Biochemical Analysis

Blood samples (2-3 mL) were collected following animal sacrifice for liver, kidney, and lipid profile assessment. Blood was collected in and centrifuged at 3000 r.p.m. for 5 minutes. The blood

biochemical parameters were measured using the commercially available kits (SPECTRUM company, Shanghai, China). Statistical significance was determined using one-way ANOVA, and $p < 0.05$ was considered significant.

2.7. Histopathological Analysis

After four weeks of treatment, rats were sacrificed, and samples collected. The liver, kidney, and pancreas samples were washed in Saline solution and post-fixed for 24 hours in 4% paraformaldehyde. Samples were dehydrated in alcohol (70%, 80%, 90%, 95%, and 100%), cleared in terpineol for 24 hours, and infiltrated in Paraplast at 60 °C for 2 hours. Finally, the tissues are embedded in paraffin wax then sectioned using Leica Rotary Microtome™ (Model: 1512). 5-6 µm thick sections are mounted on clean glass slides. Paraffin sections were deparaffinized and stained with Mayer's Hematoxylin and counterstained with 1% Eosin (H&E) (Lillie & Fullmer, 1976).

The diameter of pancreatic islets was evaluated according to the methods described by (Glaharn, Punsawad, Ward, & Viriyavejakul, 2018). An average of 40 islets for each animal was measured under 100 x using image analysis software (ImageJ, National Institutes of Health, version 1.5a). Data were presented as mean ± SD applying one-way analysis of variance (ANOVA) followed by Tukey's comparison test using GraphPad Instat (Prism). A P- a value of < 0.05 was considered to be statistically significant.

The scoring of liver and kidney damage was performed according to previous studies (Klopfleisch, 2013; Knodell et al., 1981), the grade of damage was obtained by adding the entire score of the types of histopathological lesions (4-5 field/rat/200x), as described in the appendix **Table 4.** Differences between the data were analyzed using Kruskal–Wallis test, followed by Dunn's Multiple Comparison Test. Data were expressed as median ± SD.

2.8. Statistical Analysis

Statistical analysis was performed using R software version 3.5.2 and GraphPad PRISM version 5. R software was used for the MTT analysis to determine the toxicity level for the different

concentrations. One-Way ANOVA (Analysis of Variance) for multiple comparisons among samples/groups and t-test was used to determine significance. Data are presented as mean ± SD.

Bruker Daltonics Data Analysis 4.4 was used for chromatograms inspection. While Metaboscape (Bruker Daltonics) 3.0 was used for data pre-processing using T-ReX 3D (Time aligned Region Complete eXtraction) algorithm for retention time alignment. Where isotopes, adducts, and fragments belonging to the same compound are automatically detected and combined into one feature. Detected features are displayed as a bucket table with their corresponding Rt, measured *m/z*, molecular weight, and detected fragments. The Bucket table was created with intensity threshold $10e_4$ for both negative and positive ionization modes with a retention time range from 0 to 18 min and mass range from 120 to 1600 *m/z* (Olmo-García et al., 2019).

For the molecular networking and metabolites annotation, the features list created by the Metaboscape was exported as MGF file for both of the positive and negative measurements. The negative and positive mode MGF files were uploaded independently to the GNPS online platform (https://gnps.ucsd.edu), where two molecular networks were created following the online workflow (GNPS 2.0). A molecular network was created with a cosine score above 0.65 and 0.7 for positive and negative modes, respectively, and the number of shared fragments was adjusted to 4. The networks were visualized using Cytoscape 3.5.1 (Smoot, Ono, Ruscheinski, Wang, & Ideker, 2011).

Chapter Three: Results

3.1. Results

3.1.1. (MTT) Cytotoxicity results

The methanolic extract of *Adansonia digitata L.* plant extract was tested on L-929 fibroblast cell line. The results showed very low cytotoxicity levels for the tested concentrations (10 µg/mL, 20 µg/mL, 50 µg/mL, 100 µg/mL, 150 µg/mL, and 250 µg/mL). All experiments were conducted in triplicates with 5% Dimethyl Sulfoxide (DMSO) as a positive control. The negative control consisted of cells only with no extract. A third control consisted of 0.05% DMSO, since it was the solvent used to reconstitute the extracts. Cells were examined and photographed using Olympus Inverted System Microscope Model IX70 (**Figure 9**).

The results showed that the *Adansonia digitata L.* methanolic extract is safe and did not cause cell death on the L-929 fibroblast cell line (**Figure 10)**, compared to the 5% DMSO which was very toxic. The observed IC50 for the extract was 105.7 µg/mL.

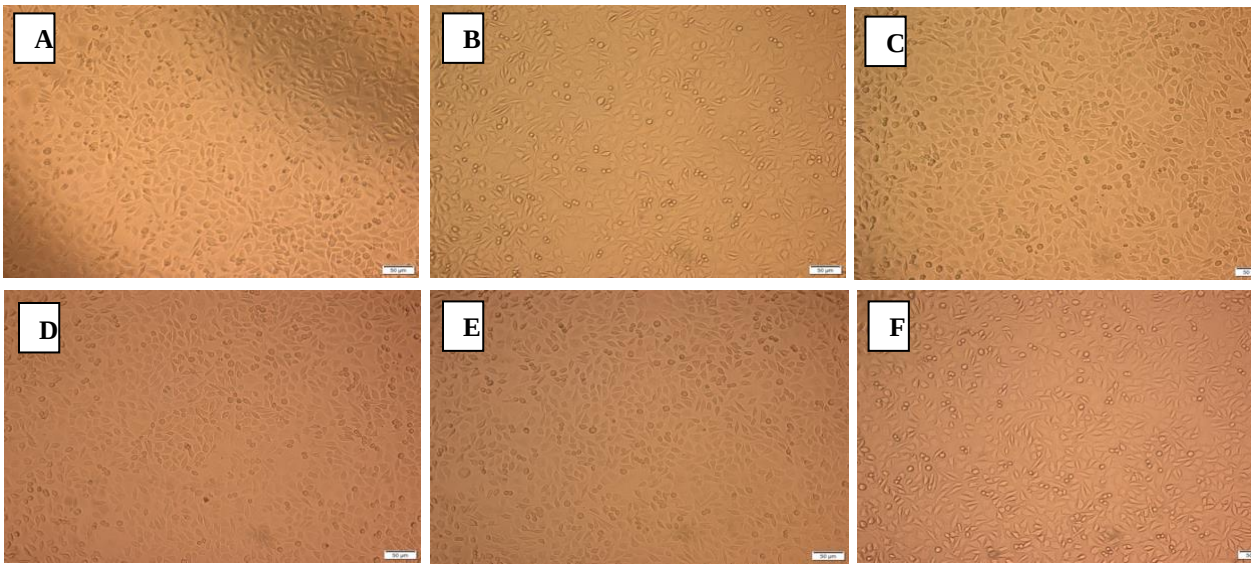

Figure 9: Cytotoxicity of *Adansonia digitata L.* fruit methanolic extract.

Photomicrographs showing L-929 cells after 24 h incubation with, under 10X magnification with a picture scale of 50 µm (Olympus Inverted System Microscope Model IX70)

A. AD/MeOH 250 µg/mL
B. AD/MeOH 150 µg/mL
C. AD/MeOH 100 µg/mL
D. AD/MeOH 50 µg/mL
E. AD/MeOH 20 µg/mL
F. AD/MeOH 10 µg/mL

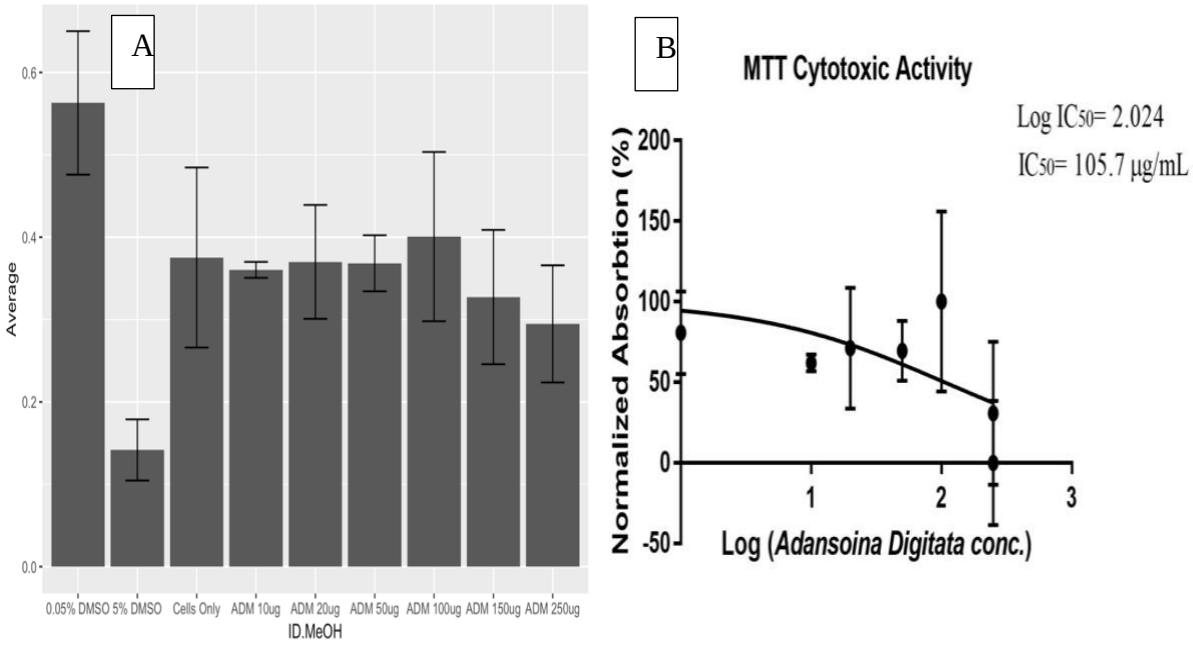

Figure 10: Cytotoxicity and IC50 of *Adansonia digitata* L. fruit extract.

(A) *Adansonia digitata L.* fruit methanolic extract MTT cytotoxicity analysis with R software version 3.5.2. (B) The IC_{50} curve with GraphPad PRISM version 6

3.1.2. Antioxidant Activity Using (DPPH) Results

The methanolic extract of *adansonia digitata L.* plant was examined to determine which extract has a higher antioxidant activity. The results showed that the methanolic extract showed high antioxidant activity. Six different concentrations of methanol extracts were tested (10 µg/mL, 20 µg/mL, 50 µg/mL, 100 µg/mL, 150 µg/mL, and 250 µg/mL). Ascorbic acid was used as a strong antioxidant agent.

The IC50 value, which is the sample concentration required for the 50% inhibition of the DPPH free radical, was measured by the DPPH absorbance versus the log of the concentrations curve as described previously (Garcia et al., 2012). The observed IC_{50} for the methanolic extract of the *Adansoina digitata L*. is 114.8 µg/mL (**Figure 11)**.

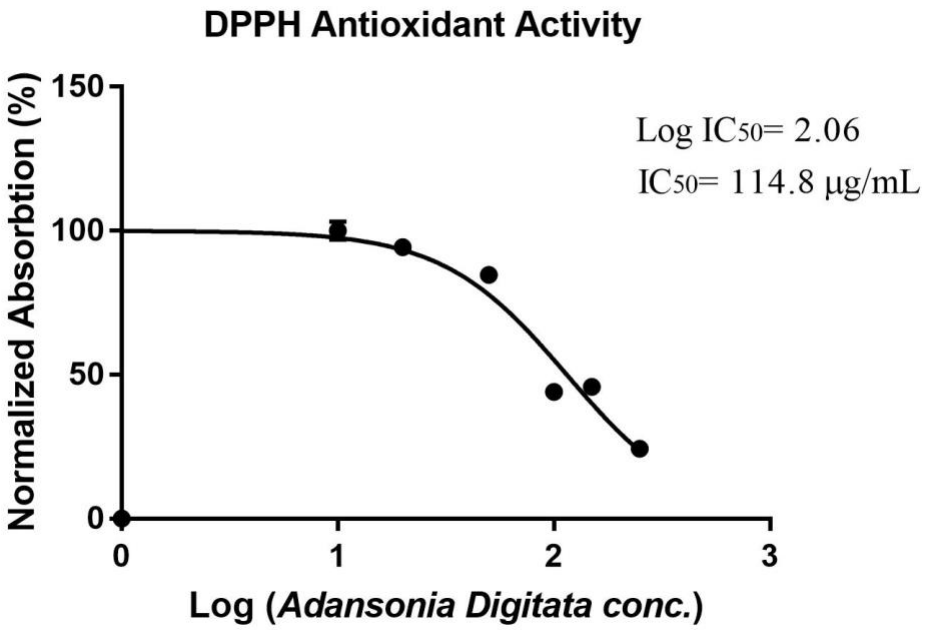

Figure 11: Antioxidant activity of *Adansonia digitata L.* methanolic extract.

DPPH antioxidant analysis IC_{50} curve with GraphPad PRISM version 6

3.1.3. UPLC-HRMS/MS profiling of *Adansonia digitata L.* fruit

Phytochemical constituents of *Adansonia digitata L.* fruits were analyzed via reversed-phase UPLC/PDA/ ESI-qTOF-MS and eluted with a gradient mobile phase, which permitted a holistic investigation of its analytes under both positive and negative ionization modes. Different ionization modes allowed for the detection of different metabolite classes through amending competitive ionization and suppression effects (M. A. Farag et al., 2016). Overlaid UPLC-MS base peak chromatogram (BPC) of *Adansonia digitata L.* fruit extract in both ionization modes is shown in **Figure 12.**

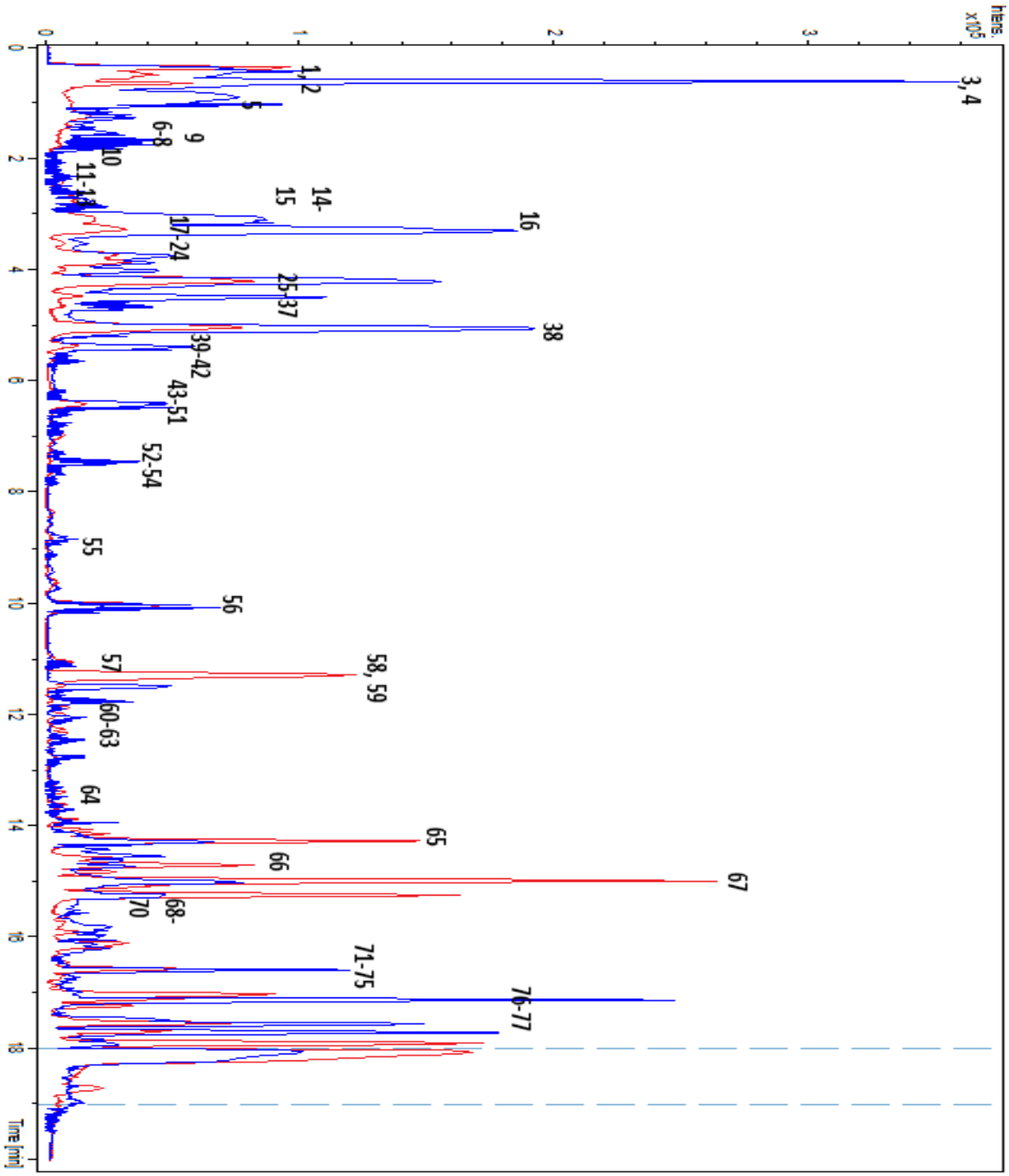

Figure 12: Overlaid BPC of *Adansonia digitata* L. fruit extract in both ionization modes.

Red and **blue** colors are corresponding to **positive** and **negative** ionization modes, respectively.

To aid in metabolite identification, two Molecular networks were generated for the positive and negative ionization modes individually through GNPS 2 platform to group peaks based on similar spectra. The spectral networks permitted the visual review of different metabolite classes, similarities among detected metabolites, and allowed isomers detection.

In contrast, the positive network exhibited 287 nodes grouped into 26 clusters and 109 single nodes, whereas the negative afforded 161 nodes in 13 clusters and 47 isolated nodes (**Figure 13**).

Molecular networking aided dereplication of *Adansonia digitata* L. metabolites

Metabolite dereplication was carried out based on their retention times, molecular formula, UV absorption maxima, and their fragmentation pattern in comparison to previously reported data. A total of 77 compounds were dereplicated belonging to different classes, including organic acids, sugars, alcohols, phenolics, coumarins, and fatty acids. Almost 50% of the identified metabolites (40 compounds) are reported for the first time in *Adonsonia digitata* fruits (Table 1). Organic acids were detected in peaks 1, 2, 5, 6, &13, while saccharides were detected in peaks 3, 4, 7, 14, 15, 25, 29, 31, &32. Aromatics were detected in peaks 8, 12, 36, 57, 60, 61, 62, benzoic acid was detected in peaks 9 &10, and the nitrogenous compound was detected in peaks 11 & 18.

In addition, flavan-3-ol was detected in peaks 16 & 28 and cinnamates were detected in peaks 17, 19, 21, 24, 26, 27, 30, 35, 37, 39, 40, 43, 50, 51, 52, 53, 63, & 64. Moreover, proanthocyanidin was detected in peaks 20, 22, 23, 33, 34, 38, & 45, furanochromones were detected only in peak 41, flavonol was detected in peaks 42, 44, 46, 47, 48, & 49, and flavonoid was detected only in peak 54. Terpenes were detected in peaks 55 & 56 and coumarin was detected in peaks 58, 59, 65, & 66. Finally, different fatty acids were detected in peaks 67, 68, 69, 70, 71, 72, 73, 74, 75, 76, & 77.

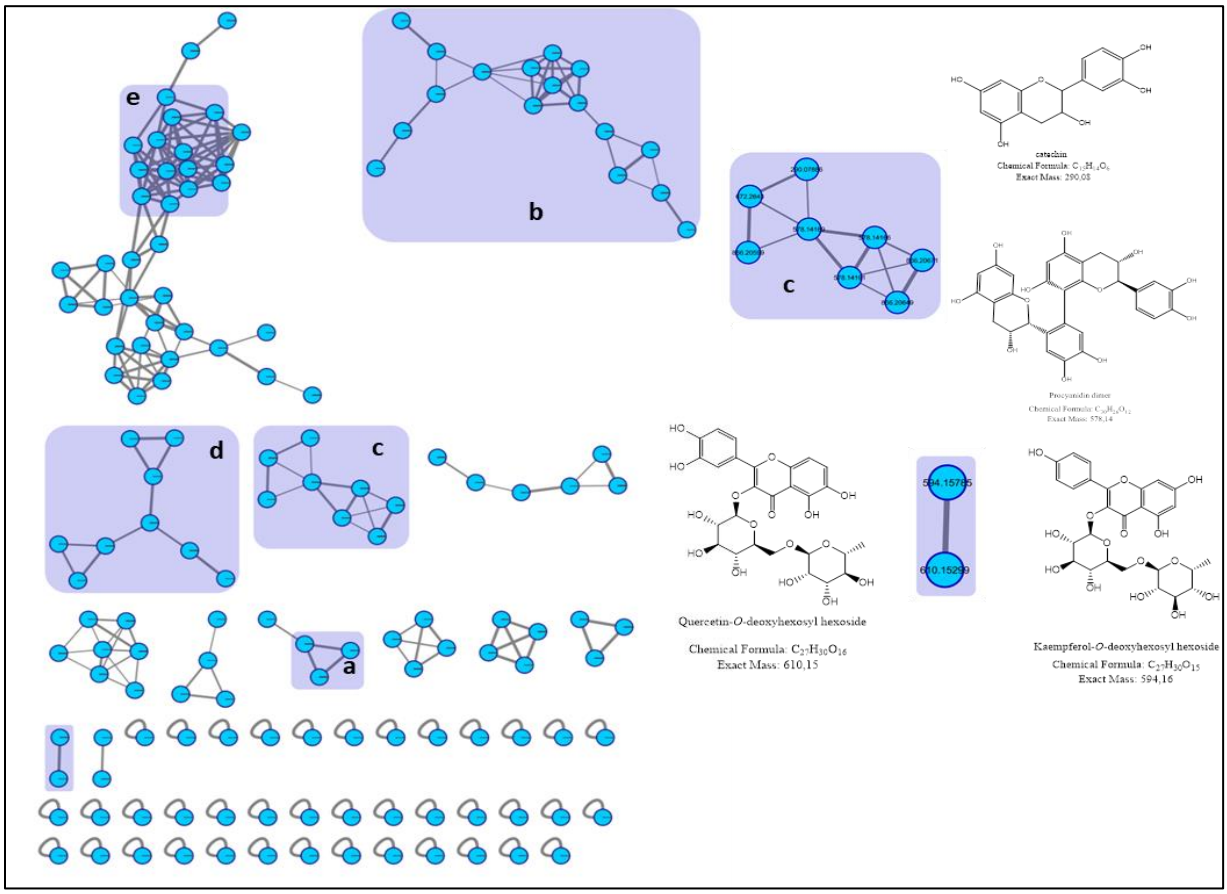

Figure 13: Negative molecular network of MS/MS data of *Adansonia digitata* L. fruit extract revealing main metabolite classes.

Table 2: The detected metabolites from the *Adansonia digitata* L. fruit using UHPLC-MS.

Peak	Rt min	Class	M-H	MS_2	M+H	MS_2	formula	Error ppm	Name	References
1.	0.48	Organic acid	191.0198	129, 111			$C_6H_8O_7$	-0.14	Citric acid	(Braca et al., 2018)
2.	0.48	Organic acid	133.0142	115			$C_4H_6O_5$	0.3	Malic acid	(Arold Jorel Tsetegho Sokeng et al., 2019)
3.	0.62	Saccharides	341.1091	179, 133	343.1234	163	$C_{12}H_{22}O_{11}$	0.06	Disaccharide (sucrose)	(Arold Jorel Tsetegho Sokeng et al., 2019)
4.	0.66	Saccharides	371.1196	325, 193			$C_{13}H_{24}O_{12}$	0.16	Unknown diasaccharide*	
5.	0.75	Organic acid	191.0200	111			$C_6H_8O_7$	-1.87	Citric acid isomer	(Braca et al., 2018)
6.	1.0	Organic acid	205.0354	111			$C_7H_{10}O_7$	-0.7	Citric acid methyl ester*	(Leenamaija Makila et al., 2016)
7.	1.3	Saccharides			385.1699	163, 145	$C_{15}H_{28}O_{11}$	1.36	Butandiol-*O*- pentoside-*O*-hexoside*	(Hui Sun et al., 2016)
8.	1.39	Aromatics			127.0393	109	$C_6H_6O_3$	-4.05	Pyrogallol*	(Hatice Tohma et al., 2017)
9.	1.53	Benzoic acid	167.0353	123			$C_8H_8O_4$	2.05	Vanillic acid*	(Gruz, Novák, & Strnad, 2008)
10.	1.82	Benzoic acid	153.0193	109	155.0342	111	$C_7H_6O_4$	-2.02	Dihydroxy benzoic acid* (protocatechuic acid)	(Ismail, Pu, Guo, Ma, & Liu, 2019)
11.	2.48	Nitrogenous compound			188.0701		$C_{11}H_9NO_2$	2.51	Unknown	
12.	2.6	Aromatics	137.0243	109			$C_7H_6O_3$	-2.6	Dihydroxybenzaldehyde*	(Lutter, Clark, Prenzler, & Scollary, 2007)
13.	2.84	Organic acid	175.0615	131, 157			$C_7H_{12}O_5$	-1.8	Hydroxyglutaric acid*	(Peter Lorenz et al., 2012)
14.	3.32	Saccharides			369.1753	295, 163, 145, 133, 115	$C_{15}H_{28}O_{10}$	0.38	Butanol-*O*-hexopyranosyl-*O*-deoxypyranoside*	(Fujimatu, Ishikawa, & Kitajima, 2003)
15.	3.32	Saccharides			295.1012	163, 145, 133	$C_{11}H_{18}O_9$	2.55	Dihydroxy-methylene-butanoate-*O*-hexoside *	Tuliposide B (I. M. Abu-Reidah, Arráez-Román, Al-Nuri,

Peak	Rt min	Class	M-H	MS_2	M+H	MS_2	formula	Error ppm	Name	References
										Warad, & Segura-Carretero, 2019)
16.	3.39	Flavan-3-ol	289.0717	245, 203	291.0861	207, 139	$C_{15}H_{14}O_6$	2.42	Catechin/ Epicatechin	(Braca et al., 2018; Ismail et al., 2019)
17.	3.5	Cinnamates	353.0891	191			C16H18O9	-2.1	*O*-Caffeoyl quinic acid ester (Clorogenic acid)	(Ismail et al., 2019)
18.	3.53	Nitrogenous compound	352.1034	191			$C_{16}H_{19}NO_8$	0.85	Unknown*	
19.	3.72	Cinnamates	281.0660	193, 163, 145			$C_{13}H_{14}O_7$	4.39	*O*-feruloyl lactic acid ester*	(S. Wu, Wilson, Chang, & Tian, 2019)
20.	3.79	Proanthocyanidin	577.1345	407, 289			$C_{30}H_{26}O_{12}$	-0.98	Procyanidn dimer isomer	Xx (Braca et al., 2018; Ismail et al., 2019)
21.	3.8	Cinnamates	327.1082	165, 147			$C_{15}H_{20}O_8$	2.8	Dihydrocoumaroyl *O*-hexoside (dihydromelilotoside)*	*(Yang et al., 2007)*
22.	3.9	Proanthocyanidin	577.0346	407, 289	579.1472	409, 301, 291	$C_{30}H_{26}O_{12}$	4.25	Procyanidn dimer isomer I	(Braca et al., 2018; Ismail et al., 2019)
23.	3.91	Proanthocyanidin	865.1987			289	$C_{45}H_{38}O_{18}$	0.2	Procyanidin trimer isomer I	(Braca et al., 2018; Ismail et al., 2019)
24.	3.98	Cinnamates	341.0893	179, 161			$C_{15}H_{18}O_9$	4.5	Caffeoyl–*O*-hexoside	(X.-N. Li et al., 2017)
25.	4.03	Saccharides			295.1018	163, 145, 133	$C_{11}H_{18}O_9$	1.88	Dihydroxy—methylenebutanoate-*O*-hexoside isomer	(I. M. Abu-Reidah et al., 2019)
26.	4.1	Cinnamates	487.1457	193			$C_{21}H_{28}O_{13}$	-1.3	Feruloyl *O*- pentosyl - *O*-hexoside*	(Ibrahim M Abu-Reidah, Arráez-Román, Segura-Carretero, & Fernández-Gutiérrez, 2013)
27.	4.23	Cinnamates			165.0544	119, 107	$C_9H_8O_3$	3.67	Coumaric acid	(Ismail et al., 2019)
28.	4.24	Flavan-3-ol	289.0716	245, 203	291.0860		$C_{15}H_{14}O_6$	-0.27	Catechin/ Epicatechin	(Braca et al., 2018; Ismail et al., 2019)
29.	4.33	Saccharides			295.1018	163, 145, 133	$C_{11}H_{18}O_9$	1.9	Dihydroxy-methylenebutanoic acid-*O*-hexoside	(I. M. Abu-Reidah et al., 2019)

Peak	Rt min	Class	M-H	MS_2	M+H	MS_2	formula	Error ppm	Name	References
30.	4.47	Cinnamates	325.0925	163			$C_{15}H_{18}O_8$	-0.29	Coumaroyl-*O*- hexoside*	(Ibrahim M Abu-Reidah et al., 2013)
31.	4.52	Saccharides			383.1905	163, 145, 133, 155	$C_{16}H_{30}O_{10}$	1.7	Methylbutyl -*O*-pentosyl-*O*-hexoside*	(I. M. Abu-Reidah et al., 2019)
32.	4.52	Saccharides			295.1008	163, 145, 133	$C_{11}H_{18}O_9$	0.9	Dihydroxy-methylenebutanoic acid-*O*-hexoside	(I. M. Abu-Reidah et al., 2019)
33.	4.52	Proanthocyanidin	865.1992	577, 407, 289			$C_{45}H_{38}O_{18}$	1.03	Procyanidin trimer Isomer II	Xx (Braca et al., 2018; Ismail et al., 2019)
34.	4.7	Proanthocyanidin	865.1994		867.1867	579, 289	$C_{45}H_{38}O_{18}$	0.77	Procyanidin trimer isomer	Xx (Braca et al., 2018; Ismail et al., 2019)
35.	4.73	Cinnamates	367.1024	191, 173, 133			$C_{17}H_{20}O_9$	-2.77	*O*-feruloyl quinic acid	Xx (Braca et al., 2018)
36.	4.8	Aromatics	461.1653	149			$C_{20}H_{30}O_{12}$	4.5	Homovanillyl alcohol-*O*-pentosyl hexoside*	(Yang Zhang et al., 2012)
37.	4.8	Cinnamates	163.0401	119			C9H8O3	-0.1	Coumaric acid isomer	(Ismail et al., 2019)
38.	5.02	Proanthocyanidin	1153.2595	865, 577, 289			$C_{60}H_{50}O_{24}$	-2.04	Procyanidin tetramer	(Ismail et al., 2019)
39.	5.1	Cinnamates			163.0391	135	$C_9H_8O_3$	-0.5	Unknown*	
40.	5.49	Cinnamates	367.1031	191, 173, 133			$C_{17}H_{20}O_9$	-0.52	*O*-feruloyl quinic acid isomer	(Braca et al., 2018)
41.	5.59	Furanochromones			409.1111	247	$C_{19}H_{20}O_{10}$	4.37	Khellol-*O*-hexoside*	(Schuster, 1980)
42.	5.66	Flavonol	609.1457	301			$C_{27}H_{30}O_{16}$	-0.65	Quercetin-*O*-deoxyhexosyl hexoside	(Braca et al., 2018)
43.	6.2	Cinnamates	325.0916	163			$C_{15}H_{18}O_8$	-3.57	Coumaroyl-O-hexoside	(X.-N. Li et al., 2017)
44.	6.27	Flavonol	609.1467	301			$C_{27}H_{30}O_{16}$	1.04	Quercetin-*O*-deoxyhexosyl hexoside	(Braca et al., 2018)
45.	6.43	Proanthocyanidin	577.1346	407, 289			$C_{30}H_{26}O_{12}$	-0.93	Procyanidn dimer isomer III	(Braca et al., 2018; Ismail et al., 2019)
46.	6.46	Flavonol			449.1073	287	$C_{21}H_{20}O_{11}$	1.17	Kaempferol-*O*-hexoside	(Braca et al., 2018)

Peak	Rt min	Class	M-H	MS_2	M+H	MS_2	formula	Error ppm	Name	References
47.	6.44	Flavonol	593.1505	447, 285	595.1617	449 , 287	$C_{27}H_{30}O_{15}$	1.04	Kaempferol-*O*-deoxyhexosyl hexoside*	(Ferreres et al., 2017)
48.	6.47	Flavonol			287.0543	217, 151	$C_{15}H_{10}O_6$	3.07	Kaempferol	(Braca et al., 2018)
49.	6.52	Flavonol	593.1505	447, 285			$C_{27}H_{30}O_{15}$	-2.46	Kaempferol-*O*-deoxyhexosyl hexoside isomer*	(Ferreres et al., 2017)
50.	6.62	Cinnamates	293.0671	163, 145, 119			$C_{14}H_{14}O_7$	1.28	*O*-coumaroyl malic acid methyl ester*	(M. K. Lee et al., 2007)
51.	6.88	Cinnamates	355.1022	193			$C_{16}H_{20}O_9$	-3.48	Feruloyl -*O*- hexoside	(X.-N. Li et al., 2017)
52.	7.3	Cinnamates	326.1032	206, 163, 145			$C_{18}H_{17}NO_5$	-0.52	Coumaroyl –*N*-tyrosine*	(Clifford & Knight, 2004)
53.	7.5	Cinnamates	279.0870	163			$C_{14}H_{16}O_6$	1.6	Unknown*	
54.	7.63	Flavonoid	447.09314	285			$C_{21}H_{20}O_{11}$	0.34	Kaempferol-*O*-hexoside	(Braca et al., 2018)
55.	8.9	Terpenes	405.2123	225			$C_{19}H_{34}O_9$	3.8	Megastigmane-*O*-hexoside*	(K. Singh, Dubey, Tripathi, Singh, & Saraf, 2014)
56.	10.1	Terpenes	507.2582	345			$C_{27}H_{40}O_9$	0.9	Unknown	
57.	11.2	Aromatics	149.0605	122			$C_9H_{10}O_2$	-1.68	Unknown	
58.	11.32	Coumarin			261.0753	230	$C_{14}H_{12}O_5$	0.36	Khellin*	(Vanachayangkul, Butterweck, & Frye, 2009)
59.	11.38	Coumarin			231.0648	203, 216	$C_{13}H_{10}O_4$	1.35	Visnagin*	(Vanachayangkul et al., 2009)
60.	12.29	Aromatics			137.0600	122, 109	$C_8H_8O_2$	-2.2	Methoxy benzaldehyde	(Razanamaro et al., 2015)
61.	12.31	Aromatics			133.0651	105	C_9H_8O	2.94	Cinnamaldehyde	(Seukep et al., 2013)
62.	12.32	Aromatics			165.0907	137, 124	$C_{10}H_{12}O_2$	1.63	Eugenol	(Razanamaro et al., 2015)
63.	13.6	Cinnamates			207.1017	165, 150	$C_{12}H_{14}O_3$	-0.9	Unknown *	
64.	13.72	Cinnamates			211.0961	193, 181, 165	$C_{11}H_{14}O_4$	1.55	Unknown*	

Peak	Rt min	Class	M-H	MS_2	M+H	MS_2	formula	Error ppm	Name	References
65.	14.97	Coumarin			411.1410 [M+Na]	329, 245, 227, 199	$C_{21}H_{24}O_7$	0.81	Isovaleryl-acetyl khellactone (dihydrosamidin)*	(Olennikov, Fedorov, Kashchenko, Chirikova, & Vennos, 2019)
66.	14.98	Coumarin			329.1377	245, 227	$C_{19}H_{20}O_5$	1.9	Decursin*	(H. J. Lee et al., 2009)
67.	15.1	Fatty acid	295.2274	277, 233			$C_{18}H_{32}O_3$	1.3	Hydroxyoctadecadienoic acid*	(Napolitano, Cerulli, Pizza, & Piacente, 2018)
68.	15.1	Fatty acid	271.2278	253			$C_{16}H_{32}O_3$	1.2	Hydroxyhexadecanoic acid*	(Feussner & Feussner, 2019)
69.	15.4	Fatty acid	269.2108	251		225	$C_{16}H_{30}O_3$	5.1	Oxohexadecanoic acid*	(Nam et al., 2019)
70.	16.1	Fatty acid	295.2271	277, 233			$C_{18}H_{32}O_3$	-3.1	Hydroxyoctadecadienoic acid*	(Liang et al., 2018)
71.	16.1	Fatty acid	297.2423				$C_{18}H_{34}O_3$		Hydroxy- octedecaenoic acid*	(Napolitano et al., 2018)
72.	16.3	Fatty acid	311.2225	293, 275, 223			$C_{18}H_{32}O_4$	1.1	Dihydroxy-octadecadienoic acid*	(Liang et al., 2018)
73.	16.6	Fatty acid	277.2171	259			$C_{18}H_{30}O_2$	1.8	Octadecatrienoic acid*	(Osman, 2004)
74.	16.93	Fatty acid	355.3216	309			$C_{22}H_{44}O_3$	0.22	Hydroxydocosanoic acid*	(Feussner & Feussner, 2019)
75.	17.1	Fatty acid	279.2331	261			$C_{18}H_{32}O_2$	-0.6	Octadecadienoic acid (linoleic acid)	(Osman, 2004)
76.	17.5	Fatty acid	279.2331	261			$C_{18}H_{32}O_2$	-1.8	Octadecadienoic acid (linoleic acid)	(Osman, 2004)
77.	17.6	Fatty acid	255.2333				$C_{16}H_{32}O_2$	-0.8	Hexadecanoic acid (palmitic acid)	(Razafimamonjison et al., 2017)

*** Metabolites detected for the first time from *Adansonia digitate L.* fruit.**

3.1.4. Biochemical Assessment

Fasting blood glucose (FBG) was assessed to determine the effect of the *Adansonia digitata L.* fruit extract on the glucose level of diabetic rats. Untreated diabetic rats showed the highest FBG level. The 150 mg/kg of the fruit extract twice/ week was able to keep the blood glucose levels of the diabetic rats within the normal range (**Figure 14)**. Unexpectedly, the high dose treatment (300 mg/kg) did not reduce the blood glucose levels, and most of the rats were above 250 mg/dL. Diabetic rats in all experimental groups gained weight throughout the experiment compared to normal healthy rats and normal rats receiving the extract.

Liver functions (ALT, AST, and Alkaline phosphatase), renal functions (Creatinine, Blood Urea Nitrogen, and uric acid), and lipid profile (Cholesterol, Triglycerides, and HDL) were tested to examine the effect of the *Adansonia digitata* L. fruit extract (**Figure 15 and Table 3).**

Liver functions and Lipid Profile

The alkaline phosphatase (ALK) was reduced to near normal (166 ± 50 U/L) in treated groups, compared to the untreated diabetic rats (559 ± 328 U/L). The ALT liver enzyme was slightly higher in the tested groups compared to the normal rats (28 ± 12.02 U/L). Untreated diabetic, metformin-treated, and *Adansonia digitata* L. extract treated rats showed high levels of ALT, compared to normal. In other words, *Adansonia digitata* L. extract did not have an effect on the ALT enzyme in the tested rats. AST liver enzyme was elevated in the untreated diabetic group compared to normal. Metformin and *Adansonia digitata* L. treated groups showed a decrease in the AST levels. *Adansonia digitata* L. administration in normal rats did not alter the ALK, ALT or AST levels.

The lipid profile was assessed by the total cholesterol, triglycerides, and high-density lipoprotein (HDL) levels. Cholesterol levels increased in diabetic rats compared to normal rats, which had cholesterol levels in range (49.5 ± 7.77 mg/dL). *Adansonia digitata* L. fruit extract significantly (p-value < 0.05) reduced the cholesterol levels in both low and high doses treatment groups (Cholesterol was 46.2 ± 8.31 mg/dL in 150 mg/kg treatments and in 300 mg/kg treatment it was 79.33±9.86 mg/dL).

Triglyceride levels were higher in metformin-treated rats compared to normal and untreated diabetic rats. *Adansonia digitata* L. fruit extract reduced TG levels in both high and low treatment groups compared to metformin-treated. HDL increased in all experimental groups compared to the normal rats. However, *Adansonia digitata* L. fruit extract administration in normal rats caused an elevation in Cholesterol, TG, and HDL.

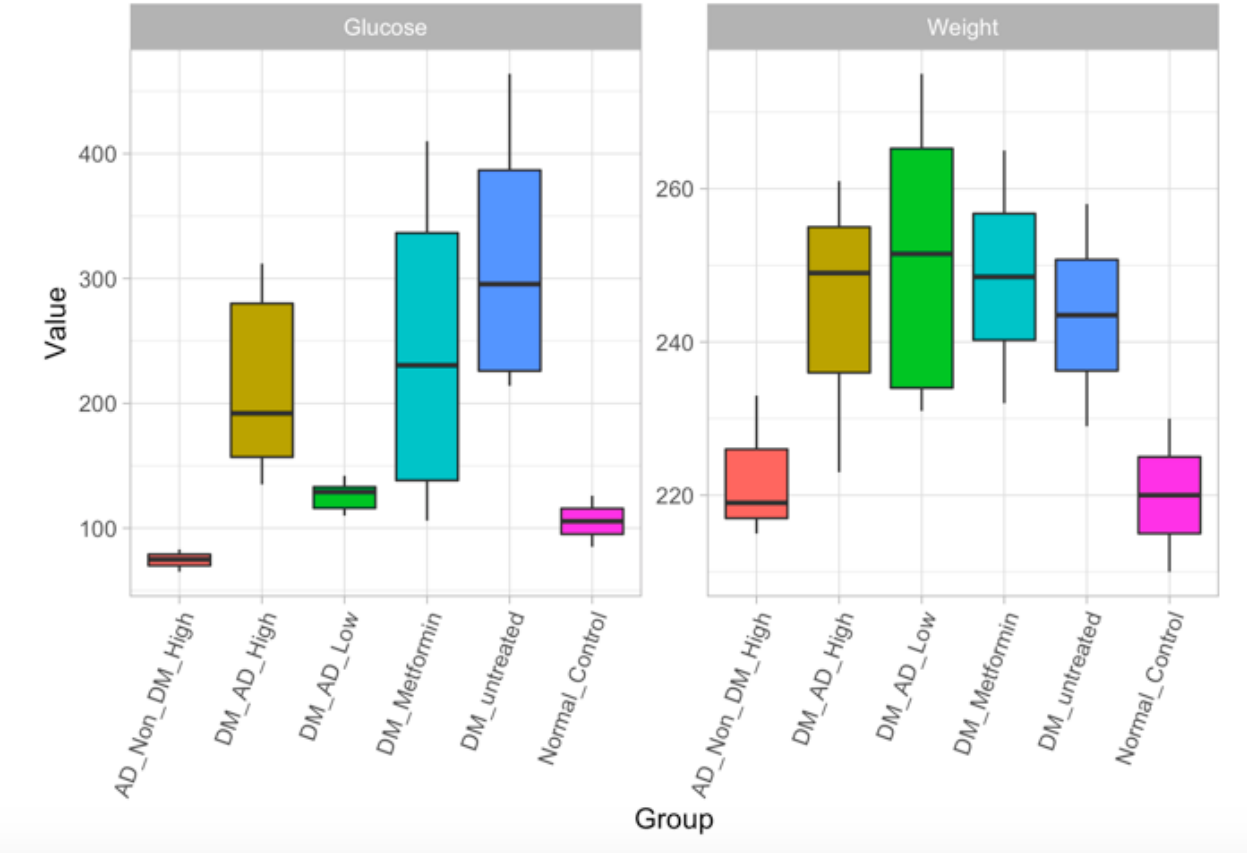

Figure 14: Fasting blood glucose (FBG) and body weight of rats.

*The fasting blood glucose result was statistically significant p-value (≤ 0.05)

Renal Functions

The results of the kidney function tests revealed that Creatinine levels were high in the metformin-treated diabetic group, as well as in the *Adansonia digitata* L. high dose (300 mg/kg) treated group. However, in the low dose of *A. digitata* (150 mg/kg) and the untreated diabetic groups, Creatinine levels were within the normal range.

Urea level was elevated in the untreated diabetic rats compared to normal control. Metformin treatment caused an insignificant reduction in the urea levels. Urea levels in the *Adansonia digitata* L. treated groups were 36.8 ± 7.49 mg/dL and 50.33 ± 11.15 mg/dL, in the low and high dose groups, respectively.

Uric acid levels increased in diabetic rats. Metformin treatment caused a significant reduction in uric acid levels. All rats receiving *Adansonia digitata* L. extract showed high levels of uric acid compared to normal healthy rats.

Table 3: Comparison of the six animal groups' blood biochemical analysis results compared to the normal healthy rats.

	Normal Healthy	DM untreated	DM + Metformin	DM + 150 mg/kg AD	Healthy + 300 mg/kg AD	DM + 300 mg/kg AD
ALT (U/L)	28 ± 12.02	37.5 ± 5.19	34 ± 15.87	32.6±11.2	34.66 ± 9.8	35.2 ±8.40
AST (U/L)	99 ± 16.97	115.75 ± 30.20	82.75 ± 33.52	83.2±13.66	94.66±19.5	69.8±12.47
Alkaline phosphatase (U/L)	166 ± 50	559 ± 328	200 ± 76	215 ± 71	364 ± 35	242 ± 56
Creatinine (mg/dL)	0.585 ± 0.049	0.49 ± 0.027	0.69 ± 0.11	0.54±0.099	0.55 ± 0.125	0.63 ± 0.11
Urea (mg/dL)	37 ± 1.414	71.75 ± 13.94	64.75 ± 29.41	36.8 ± 7.49	50.33±11.15	34.2 ± 7.19
Cholesterol (mg/dL)	49.5 ± 7.77	87.5 ± 22.98	73.5 ± 24.90	46.2 ± 8.31	79.33±9.86	55 ± 15.16
TG (mg/dL)	53.5 ± 3.53	84.75 ± 26.11	134.5 ± 73.66	87.8±25.03	116.33±66.5	110.6±26.8
HDL (mg/dL)	32 ± 12	41 ± 13	42 ± 17	46 ± 7.3	43 ± 11	47 ± 8.1
Uric Acid (mg/dL)	0.95 ± 0.77	2.22 ± 0.35	0.74 ± 0.30	2.32 ± 1.47	2.16 ± 0.61	2.30 ±1.02

*The results are expressed as the mean ± standard error (n=6).
The ALK, cholesterol, TG and urea biochemical parameters were statistically significant, p-value (≤ 0.05), the test was performed using R software version 3.5.2

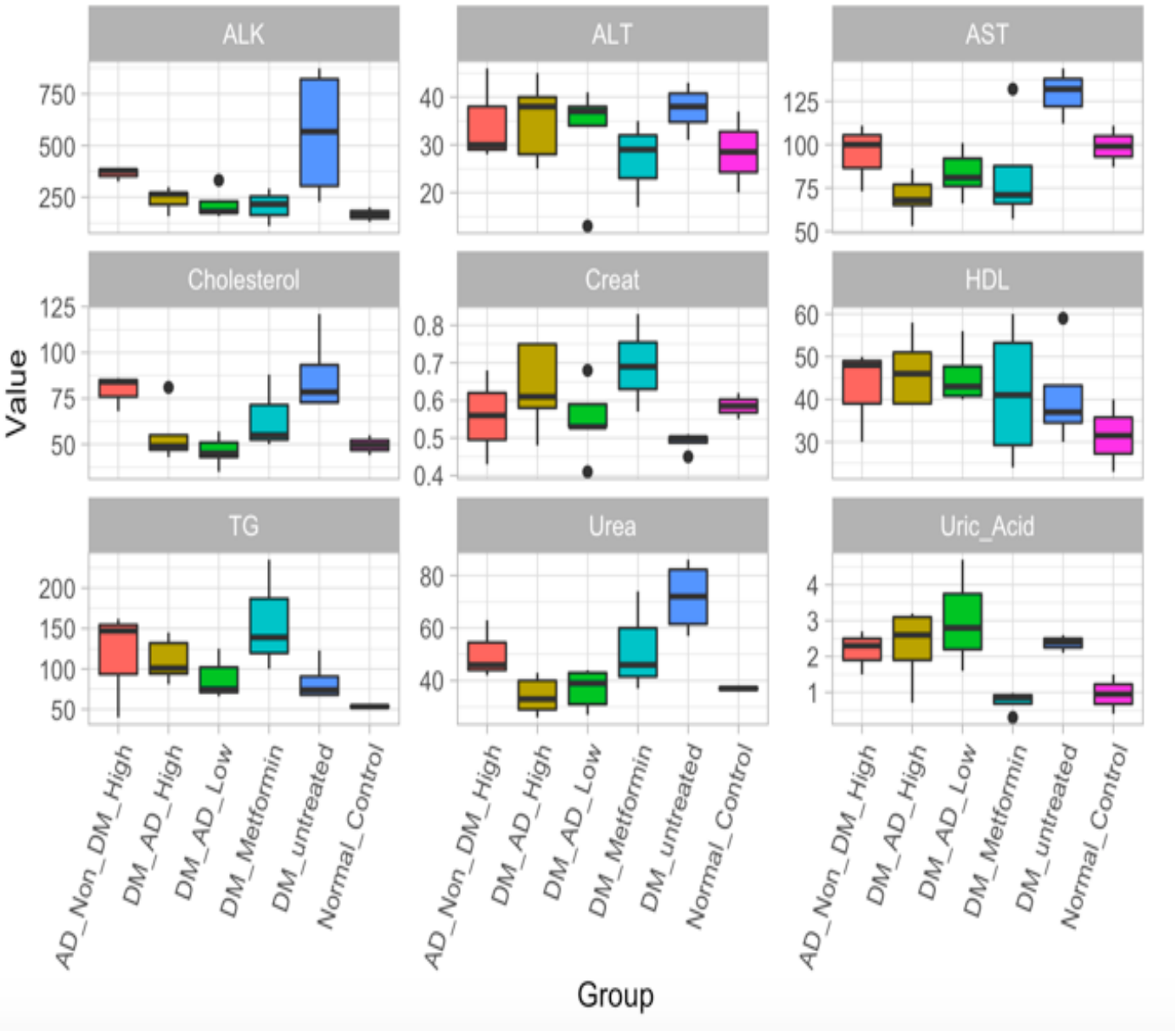

Figure 15: Biochemical analyses of the lipid profile, liver, and kidney functions.

Results of biochemical analyses in the experimental groups. The groups are normal healthy rats (Normal_Control), diabetic rats without any treatment (DM_untreated), diabetic rats administrated metformin orally (DM_Metformin), diabetic rats i.p. injection with a low dose, which is 150 mg/kg, of *Adansonia digitata* L. (DM_AD_Low), diabetic rats i.p. injection with high dose, which is 300 mg/kg, of *Adansonia digitata* L. (DM_AD_High), and healthy rats i.p. injection with high dose of *Adansonia digitata* L. (AD_Non_DM_High). Figure generated with R software version 3.5.2.

3.1.5. Histopathological Analysis

Pancreas, kidney, and liver tissues from each group (n = 9 slides/rat) were stained with hematoxylin and eosin (H&E) and examined on Olympus BX43 light microscope attached with a digital camera (DP27) and CellSens dimensions software.

Histopathology of the Pancreas

Pancreatic tissue from the normal control and normal rats that received a high dose of *Adansonia digitata* L. revealed a normal histological structure. The untreated diabetic group showed shrinkage of pancreatic islets, severe necrosis of ß-cells, and reduction in islets cell number. Similar changes were observed in the metformin-treated diabetic group. However, rats from *Adansonia digitata* L. treated diabetic groups (both low dose, 150 mg/kg and high dose, 300 mg/kg) showed an increase in islets cell numbers with normal appearance of most cells (**Figure 16**).

Histological scoring of the pancreatic islets diameter (**Figure 17**), revealed that the largest diameter was recorded in normal controls and non-diabetic rats that received a high dose of *Adansonia digitata* L. While the smallest diameter was recorded in untreated diabetic rats and diabetic rats treated with metformin, respectively.

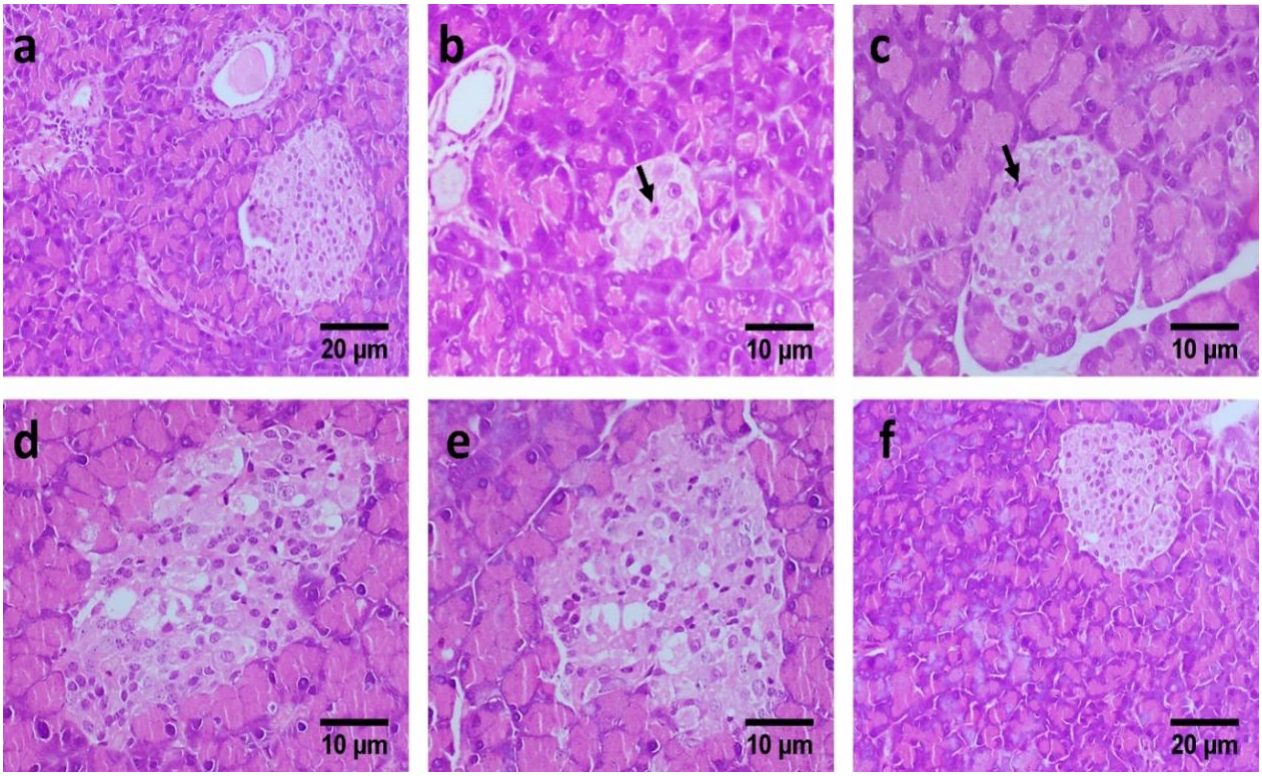

Figure 16: Histopathology of the Pancreas.

Photomicrographs of the pancreas stained by (H&E). (a) Healthy control group showing a normal histological structure of the pancreas with a regular outline of pancreatic islets. (b) DM_Untreated group showing a reduction in both the size of pancreatic islets and the number of the islets cells with necrobiotic changes (arrow). (c) DM_metformin group showing a similar pathological alteration detected in the untreated diabetic group. (d) DM_AD_Low group showing a normal appearance of islets with an increase in both islet diameter and number of islet cells. (e) DM_AD_High group showing improvement in the histological structure and number of the cells of the islets compared to the control group. (f) AD_Non_DM_High group showing a normal histological structure of both endocrine and exocrine portion.

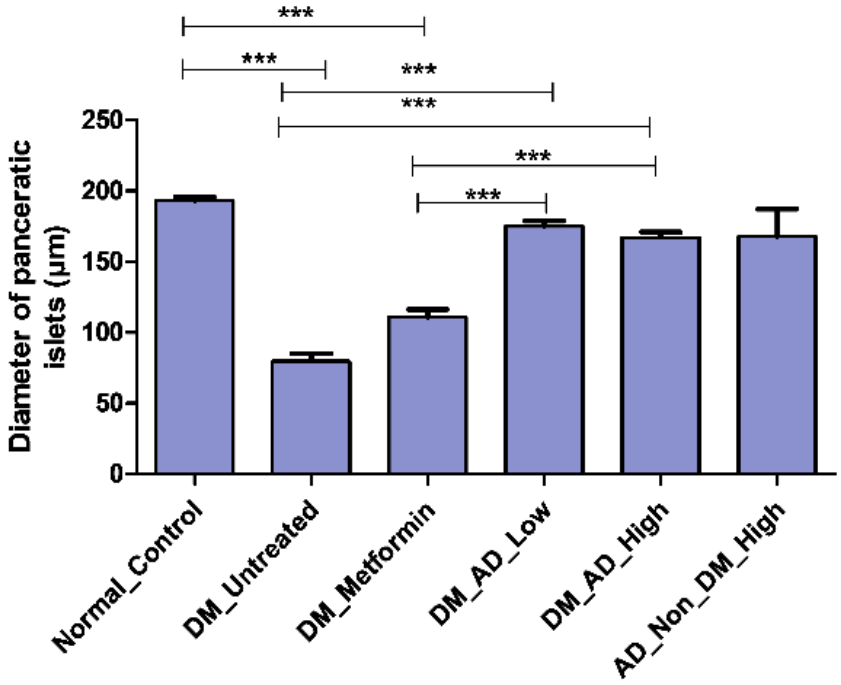

Figure 17: Histological scoring of the diameter of the pancreatic islets (µm).

Data expressed as mean ± SD. ***Significant difference between groups, P < 0.001

Histopathology of the Liver

Histological examination of liver sections of the healthy control rats (**Figure 18**) and non-diabetic rats receiving the high dose of *Adansonia digitata* L showed normal histological structure. The untreated diabetic group showed necrosis of hepatocytes adjacent to the central vein associated with inflammatory cell infiltration. In untreated diabetic rats, inflammation, necrosis, and vacuolar degeneration were detected. Liver sections from metformin-treated diabetic rats showed similar histopathological changes to the untreated diabetic group. Treatment with *Adansonia digitata* L. in both low (150 mg/kg) and high (300 mg/kg) doses, improved the histological structure of the liver. Histological score of liver lesions (**Figure 19**), showed a significant increase in tissue damage in both untreated diabetic and the metformin-treated diabetic groups (**$P < 0.01$, ***$P < 0.001$).

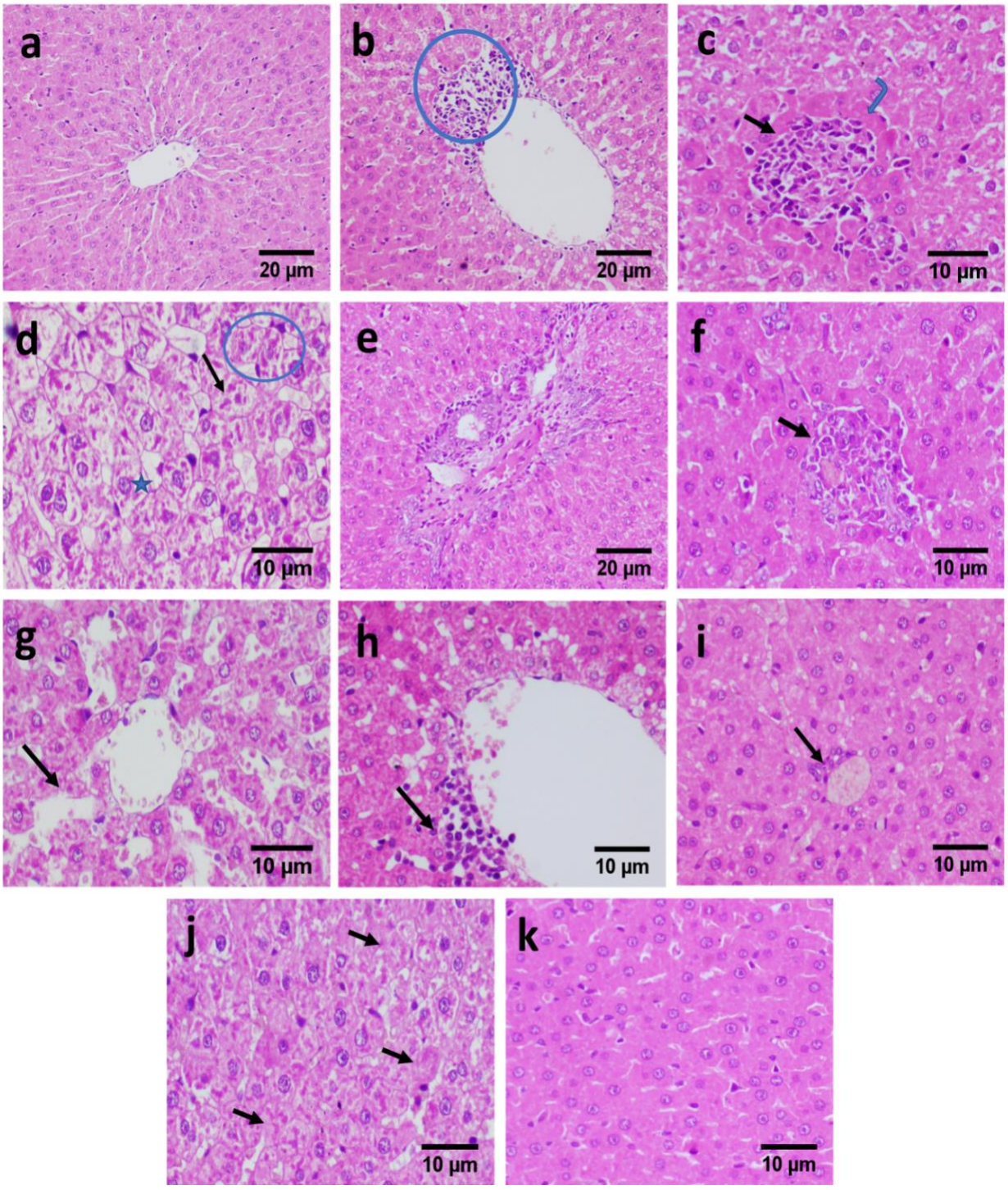

Figure 18: Histopathology of the Liver.

Photomicrographs of liver sections stained by (H&E). (a) Control group showing normal histological structure. (b) DM- untreated group showing necrosis of hepatocytes adjacent to central

vein associated with infiltration of inflammatory cells (circle), (c) focal area of necrosis associated with inflammatory cell infiltration (black arrow) as well as coagulative necrosis in the hepatocytes (blue curved arrow), (d) vacuolar degeneration (asterisk) and karyorrhexis (fragmentation of nucleus) in some hepatocyte (circle) and (e) inflammation of the portal area. (f) DM_Metformin group showing a focal area of necrosis associated with inflammatory cells infiltration (arrow), (g) vacuolar degeneration with dilation in sinusoid (arrow), and (h) infiltration of the inflammatory cell adjacent to the central vein (arrow). (i) DM_AD_Low group showing the restoration of cellular structure with minimal infiltration of inflammatory cells (arrow). (j) DM_AD_High group showing slight granulation of hepatic cytoplasm with necrosis of minute cluster of hepatocytes (spotty necrosis), (arrows). (k) AD_Non_DM_High group showing a normal cellular structure of hepatocytes.

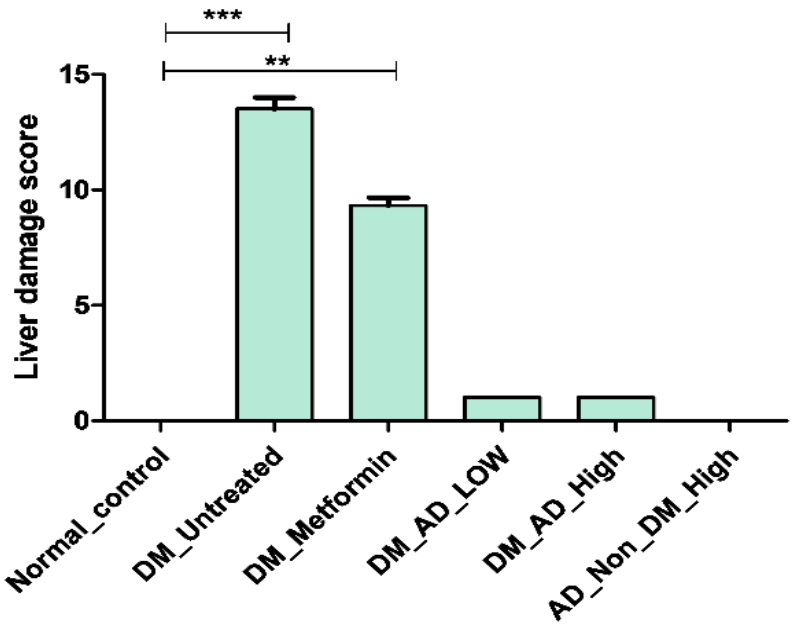

Figure 19: Histological damage score in liver tissue.

Data presented as median ± SD. **P < 0.01, ***P < 0.001.

Histopathology of the Kidney

Normal histology of the kidney was seen in the healthy control group (**Figure 20**). Vacuolar degeneration, necrobiotic changes, and interstitial nephritis were observed in the untreated diabetic group. Kidney sections from the metformin-treated group showed degenerative and necrobiotic changes in renal tubules. Treatment of diabetic rats with low (150 mg/kg) or high (300 mg/kg) dose of *Adansonia digitata* L. improved the histological structure of the kidney, and no inflammation or necrosis was observed. No histological changes were detected in normal rats receiving a high dose of *Adansonia digitata* L. fruit methanolic extract.

Scoring of kidney damage is shown in (**Fig. 21**). A significant increase in renal damage score was detected in the untreated diabetic group and metformin-treated diabetic rats when compared with the control group. There was no significant difference between diabetic rats treated with either low or high doses of *Adansonia digitata* L. fruit methanolic extract (**$P < 0.01$, ***$P < 0.001$).

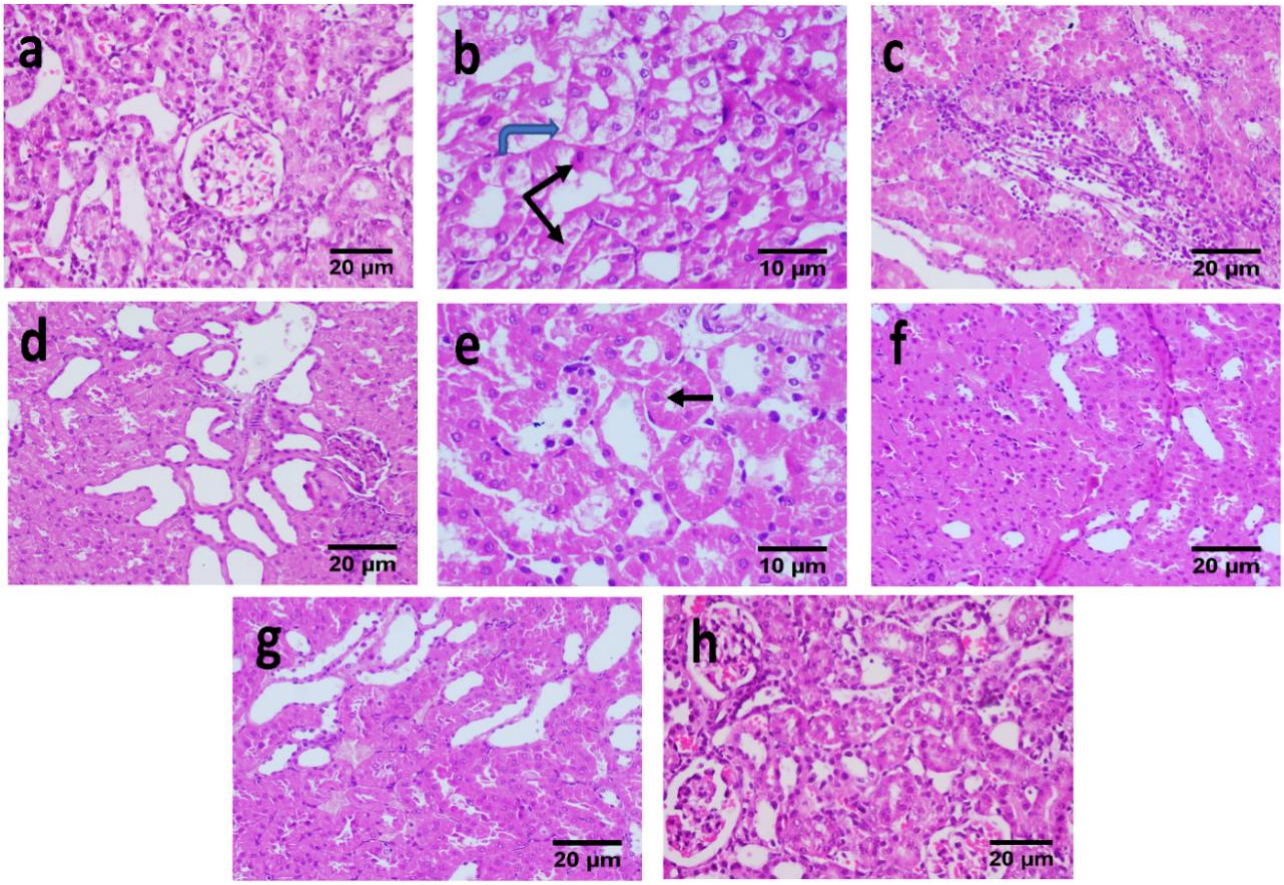

Figure 20: Histopathology of the Kidney.

Photomicrographs of **kidney** sections stained by (H&E). (**a**) Control group showing normal histological structure. (**b**) DM_Untrated group showing vacuolar degeneration of tubular epithelium (blue curved arrow) with necrobiotic changes (**black arrows**) and (**c**) Interstitial nephritis which characterized by infiltration of inflammatory cells between renal tubules. (**d**) DM_Metformin group showing cloudy swelling of tubular epithelium associated with dilation of some renal tubules and (**e**) necrobiotic changes in the epithelium lining renal tubules (**arrow**). (**f**) DM_AD_Low group showing cloudy swelling. (**g**) DM_AD_High group showing a similar change in the rats treated with a low dose of *Adansonia digitata* L. h) AD_Non_DM_High group showing normal cellular architecture.

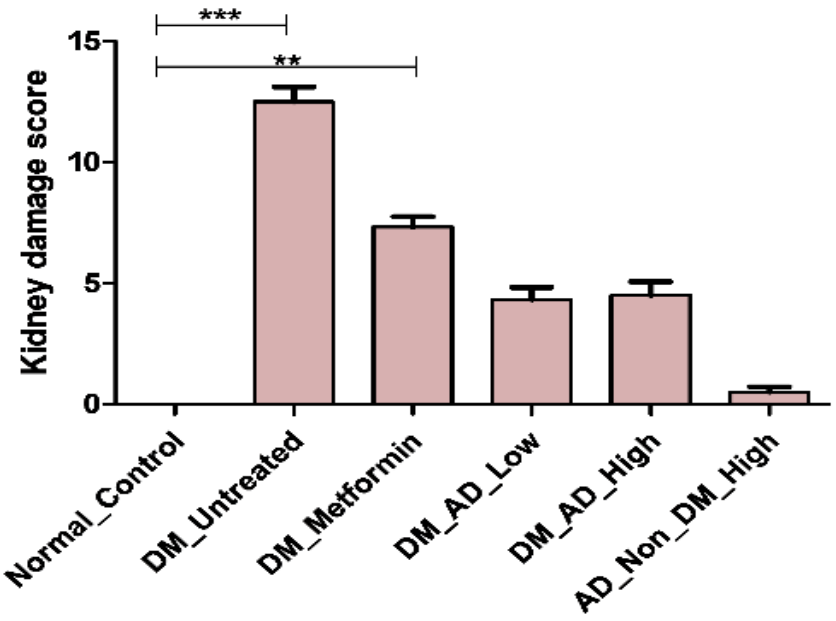

Figure 21: Histological damage score in kidney tissue.

Data presented as median ± SD. $^{**}P < 0.01$, $^{***}P < 0.001$.

Chapter Four: Discussion

Diabetes Mellitus (DM) is considered one of the fast growing diseases around the world (Soltesz, Patterson, & Dahlquist, 2007). The search for an effective anti-diabetic medication is never stopping. In this study, we assessed the anti-diabetic potential of *Adansonia digitata* L. methanolic fruit extract. Baobab or *Adansonia digitata* L. is a traditional folk medicinal plant common to Africa. In 2008, the Baobabs plant obtained EU regulatory approval as a food additive (Agency, 2002).

One of the main challenges when using a new drug or plant extract is to assess its toxicity. The MTT assay is a quantitative, sensitive, and reliable colorimetric assay (Riss et al., 2016). The *Adansonia digitata L.* plant extract showed an IC_{50} equals 105.7 µg/mL, which indicates a substantial safety margin for the tested plant extract.

The toxicity of The *Adansonia digitata* L. plant extract was also assessed *in vivo* by administering 300 mg/kg (the highest dose in the current study) to normal healthy rats. *Adansonia digitata L.* administration in normal rats did not alter the body weight, serum glucose, or liver functions (ALK, ALT, or AST levels). Urea and Creatinine were not affected in normal rats. However, all rats receiving *Adansonia digitata L.* extract showed high levels of uric acid compared to normal healthy rats, which indicates a possible side effect of using the extract in the long term. No histological changes were detected in normal rats receiving high doses of *Adansonia digitata* L. fruit extract. The liver, kidneys, and pancreas appeared normal with healthy cellular architecture, confirming the biochemical results that show the safety of the extract.

One of the advantages of using natural plant extracts is their multi-potential. In addition to its anti-diabetic activity, *Adansonia* possesses natural antioxidant properties. These natural antioxidants are essential because of their health maintenance effects, as well as their anti-aging effect (J. F. Weiss & Landauer, 2003). The observed DPPH IC_{50} for *Adansonia digitata L.* methanolic fruit extract in this study was 114.8 µg/mL. The low IC_{50} value indicates higher antioxidant activity. The current finding is consistent with previous findings that examined the methanolic extract of *Adansonia digitata L.* Stem, leaf, fruit pulp, and seed (S. Vertuani et al., 2011).

The *Adansonia digitata* L. fruit methanolic extract was tested *in-vivo* for its anti-diabetic potential. At low doses, the extract reduced fasting blood glucose (FBG) levels, and surprisingly, higher doses were not as effective. The current findings are similar to those reported by Gwarzo and Bako (2013). They found that *Adansonia digitata L.* fruit pulp (300 mg/kg) administered orally reduced blood glucose levels in Alloxan diabetic Wistar rats.

Histological examination of the pancreatic tissue confirmed the diabetic state of the rats. Untreated diabetic rats showed shrinkage of pancreatic islets and severe necrosis of ß-cells. Treatment with *Adansonia digitata* L. (both low, 150 mg/kg, and high dose, 300 mg/kg) improved the islet cell numbers with the healthy appearance of most cells. Metformin, on the other hand, did not cause a histological improvement of the pancreatic tissue.

The *Adansonia digitata L.* fruit extract did not affect body weight. All diabetic rats gained weight compared to healthy rats. To the best of our knowledge, no reported studies are discussing the effect of the fruit pulp extract on the weight in animal models of diabetes.

Liver enzymes are biochemical markers used to indicate hepatocyte necrosis and inflammation (Reichling & Kaplan, 1988). The alkaline phosphatase (ALK) was reduced to normal levels in treated groups compared to the untreated diabetic rats. The ALT liver enzyme was slightly higher in the tested groups compared to the normal rats. *Adansonia digitata L.* extract did not affect the ALT enzyme in the tested rats. *Adansonia digitata L.* and Metformin decreased the AST levels. *Adansonia digitata L.* administration in normal rats did not alter the ALK, ALT or AST levels.

The current results are consistent with those previously reported that stem bark extract of the *Adansonia digitata L.* reduced the ALK enzyme following oral administration of 200 mg/kg and 400 mg/kg (Adeoye & Bewaji, 2018).

The biochemical results are consistent with the histological findings. Both revealed that the injection of *Adansonia digitata* L. in both low (150 mg/kg) and high (300 mg/kg) doses improved the histological structure of the liver in diabetic rats.

The lipid profile was assessed by the total cholesterol, triglycerides, and high-density lipoprotein (HDL) levels. Cholesterol levels increased in diabetic rats compared to normal rats. *Adansonia digitata L.* extract significantly reduced the cholesterol and TG levels in both low and high dose

treatment groups. HDL increased in all experimental groups compared to the normal rats. However, *Adansonia digitata L.* fruit extract administration in normal rats caused an elevation in Cholesterol, TG, and HDL.

These results are contradictory with previous reports regarding the used doses Bako et al. (2014) that the fruit extract of *Adansonia digitata L.* reduced the cholesterol, triglycerides, and low-density lipoprotein LDL in alloxan diabetic Wistar rat model with the high dose 300 mg/kg. However, we are reporting that the low dose which is 150 mg/kg was more effective than the reported 300 mg/kg. On the other hand, the fruit crude extract in the current study and in previously reported findings was able to enhance the high-density lipoprotein (HDL), which is considered good cholesterol (Jomard & Osto, 2020), which is associated with a decrease in coronary risk (Bako et al., 2014; Luka & Tijjani, 2013).

Three biochemical parameters assessed kidney functions; Creatinine, Urea, and uric acid (Suliman, Osman, Abdoon, Saad, & Khalid, 2020). Creatinine levels were high in the metformin-treated diabetic group, and in the *Adansonia digitata L.* high dose (300 mg/kg) treated group indicating impairment of the renal function (Amartey, Nsiah, & Mensah, 2015). However, following the low dose of *Adansonia* (150 mg/kg), Creatinine levels were within the normal range.

Urea levels increased in the untreated diabetic rats compared to normal control. Metformin treatment and *Adansonia digitata L.* treatment reduced Urea levels indicating recovery of the renal function after treatment.

Uric acid levels increased in diabetic rats. Metformin treatment caused a significant reduction in uric acid levels. However, all rats receiving *Adansonia digitata L.* extract showed high levels of uric acid compared to normal healthy rats. This indicates a possible side effect of the use of *Adansonia digitata L.* extract.

The biochemical results were consistent with the histological examination, which showed that the treatment of diabetic rats with *Adansonia digitata* L. reversed the histological damage of the kidneys in diabetic rats.

Metabolites characterization

Compared to targeted analysis, metabolomics targets a large subset of metabolites within the biological system (Cevallos-Cevallos, Reyes-De-Corcuera, Etxeberria, Danyluk, & Rodrick, 2009). Liquid chromatography-mass spectrometry (LC-MS) is an advanced technique for the assessment of residues. LC has a universal separation mechanism which can be used for profiling secondary metabolites (Masia, Suarez-Varela, Llopis-Gonzalez, & Pico, 2016)

Recently, the chromatographic performance has been shifted to the ultra-performance liquid chromatography (UPLC), owing to its better separation efficiency (Jansson, Pihlström, Österdahl, & Markides, 2004; Klein & Alder, 2003).

Recent studies showed that the phytochemical analyses for the methanolic extract showed the presence of glycosides, flavonoids, tannins, saponins, terpenoids, and steroids. In addition, this methanolic extract from the fruit pulp showed anti-diabetic effects in Alloxan induced diabetes models (Gwarzo & Bako, 2013).

To characterize metabolites in the fruit extract, UHPLC-MS was employed for metabolites profiling. The UHPLC/MS results in **Table 2** showed several chemical classes.

Organic acids such as Citric acid and its isomer were detected in peaks 1 & 5 with [M-H]- at m/z 191.0198, $C_6H_8O_7$, and characteristic fragment at m/z 111. The negative molecular network revealed a directly correlated ion at peak 6 [M-H]- 205.0354, $C_7H_{10}O_7$, with a mass difference of 14 Da (CH_2). It was annotated as citric acid methyl ester (L. Makila et al., 2016). Other organic acids included peak 2 at m/z [M-H]- 133.0142, $C_4H_6O_5$ annotated as malic acid and peak 13 at m/z with [M-H]- 175.0615, $C_7H_{12}O_5$ and daughter ions at m/z 157 and 131 for the loss of water and CO_2 annotated as hydroxyglutaric acid (P. Lorenz et al., 2012).

Saccharides and their derivatives from which peaks **3** & **4** corresponded to two disaccharides, where **3** exhibited molecular ion [M-H]- at *m/z* 341.1107, $C_{12}H_{22}O_{11}$ and were assigned as sucrose

previously identified in *Adansonia* fruits (A. J. T. Sokeng et al., 2019) while, **4,** unknown disaccharide had [M-H]- 371.1196, $C_{13}H_{24}O_{12}$.

Butanediol-pentosyl-hexoside, peak **7** in the positive mode, showed a molecular ion at *m/z* 385.1699 $[M+H]^+$, $C_{15}H_{28}O_{11}$ (H. Sun et al., 2016). Similarly, peak **14** showed a molecular ion at *m/z* 369.1753 $[M+H]^+$, $C_{15}H_{28}O_{10}$, and a fragment at *m/z* 295 for the loss of C_4H_9O was assigned as butanol-pentosyl-hexoside (Fujimatu et al., 2003).

Additionally, the positive molecular network revealed the presence of 4 isomers of acylated hexoses; peaks **15**, **25**, **29** & **32,** which shared a molecular ion at *m/z* 295.1018 $[M+H]^+$ and corresponded to the elemental composition of $C_{11}H_{18}O_9$. Manual inspection of their MS_2 spectra showed the occurrence of a common fragment ion at *m/z* 133 resulting from the cleavage of a hexose moiety. Thus they were assigned as dihydroxy-methylenebutanoic acid-*O*-hexoside isomers (I. M. Abu-Reidah et al., 2019), which are well recognized for their antibacterial properties (Shigetomi, Shoji, Mitsuhashi, & Ubukata, 2010). While peak 31, with $[M+H]^+$ *at m/z* 383.1905, $C_{16}H_{30}O_{10}$ was found within the same cluster and was annotated as methylbutyl -*O*-pentosyl-hexoside (I. M. Abu-Reidah et al., 2019).

Several aromatic metabolites were detected sparsely in both ionization modes and revealed themselves mostly as single nodes within both spectral networks. The first eluted at peak **8** $[M+H]^+$ at *m/z* 127.0393, $C_6H_6O_3$ with a fragment at *m/z* 109 accounting for the loss of H_2O and annotated as pyrogallol (H. Tohma et al., 2017). Following at peak **12** was dihydroxybenzaldehyde with [M-H]- at *m/z* 137.0243, $C_7H_6O_3$, and a characteristic fragment at m/z 109 for the cleavage of CO (Lutter et al., 2007). Lately eluted, peak **36** *m/z* 461.1653 [M-H]- $C_{20}H_{30}O_{12}$ and showing a daughter ion at m/z 149 [M-H-162-132]- suggesting for the loss of a hexoside and pentoside and further dehydration (Y. Zhang et al., 2012). Hence, it was annotated as homovanillyl alcohol-*O*-pentosyl –*O*-hexoside.

Following, methoxy benzaldehyde, eluted at peak **60** with a molecular ion at m/z 137.0600 $[M+H]^+$, $C_8H_8O_2$, and fragment ion at *m/z* 122 and 109 for the consecutive cleavage of CH_3 and CO (Razanamaro et al., 2015). Similarly, peaks **61 & 62** with $[M-H]^+$ at *m/z* 133.0651, C_9H_8O, &

165.0907, $C_{10}H_{12}O_2$ and fragments at *m/z* 105 & 137 accounting for the loss of CO were annotated as cinnamaldehyde (Seukep et al., 2013) and eugenol (Razanamaro et al., 2015), respectively.

Several reports have demonstrated the beneficial effects of cinnamaldehyde in diabetes management. For instance, it improves glucose uptake and increases insulin sensitivity, increases glycogenesis, and reduces gastric emptying rate (Zhu et al., 2017). Additionally, eugenol is reported to exert antidiabetic activity via suppressing intestinal α-glucosidase and inhibiting sugar binding to serum albumin (P. Singh et al., 2016).

The presence of benzoic acids in *A. digitata* fruits was previously reported (Ismail et al., 2019) and were scarcely detected in peak **9** assigned as vanillic acid from its $[M-H]^-$ at *m/z* 167.0353, $C_8H_8O_4$ and fragment at *m/z* 123 $[M-H-44]^-$ for the loss of CO_2 (Gruz et al., 2008). While peak **10** at *m/z* 153.0193 $[M-H]^-$, $C_7H_6O_4$ and fragment at *m/z* 109 for the loss of CO_2 was annotated as dihydroxy benzoic acid. Benzoic acids, specifically vanillic acid, proved to protect against hyperglycemia and hyperlipidemia (Chang et al., 2015).

Cinnamates were detected at peaks **27** & **37**, and were annotated as hydroxycinnamic acid, coumaric acid isomers as concluded from their molecular ions at *m/z* 163.0401 $[M-H]^-$, 165.0544 $[M+H]^+$ and formula of $C_9H_8O_3$ (Ismail et al., 2019). Coumaric acid showed beneficial effects in the management of metabolic disorders *via* reducing serum glucose, cholesterol, and triglycerides levels (Amalan, Vijayakumar, Indumathi, & Ramakrishnan, 2016).

Quinic acid esters were detected in peak **17** annotated as *O*-caffeoyl quinic acid ester (chlorogenic acid) and **35** & **40** as 2 positional isomers of *O*-feruloyl quinic acid. Peak **17** exhibited a molecular ion at *m/z* 353.0891 $[M-H]^-$, $C_{16}H_{18}O_9$ and a base peak at *m/z* 191 suggesting *O*-caffeoyl quinic acid ester (chlorogenic acid) (Ismail et al., 2019). While peaks **35** & **40** showed *m/z* 367.1024 $[M-H]^-$, $C_{17}H_{20}O_9$ and a base peak at *m/z* 191 confirming their assignment as *O*-feruloyl quinic acid esters. Chlorogenic acids showed the capability to reduce fasting plasma glucose and glycosylated hemoglobin (Jin et al., 2015).

Other cinnamic esters included peak **19** assigned as *O*-feruloyl lactic acid at *m/z* 281.0660 [M-H]-, $C_{13}H_{14}O_7$ and yielding daughter ions at *m/z* 193 for the loss of lactic acid moiety ($C_3H_6O_3$) (S. Wu et al., 2019). Peak **50** with a molecular ion at *m/z* 293.0671 [M-H]-, $C_{14}H_{14}O_7$ and fragments at *m/z* 163 [M-H- 130]- for the cleavage of $C_5H_6O_4$ (methyl malic acid) and *m/z* 145 & 119 for dehydration and decarboxylation was tentatively annotated as *O*-coumaroyl malic acid methyl ester (M. K. Lee et al., 2007). Another coumaroyl tyrosine conjugate was detected in peak **52** at *m/z* 326.1032 [M-H]- and yielding fragments at *m/z* 206 for tyrosine and subsequent fragments at *m/z* 163 and 145 for deamidation and dehydration (Clifford & Knight, 2004).

Five cinnamoyl glycosides were identified in peaks **21**, **24**, **30**, **43**, **51**, to show fragment ions [M-H-162]- indicative of a hexoside moiety. Peak **21** was annotated as dihydrocoumaroyl *O*- hexoside (dihydromelilotoside) at *m/z* 327.1082 [M-H]-, $C_{15}H_{20}O_8$ (Yang et al., 2007). While peak **24** as caffeoyl acid *O*- hexoside showing a molecular ion at *m/z* 341.0893 [M-H]-, $C_{15}H_{18}O_9$ (X.-N. Li et al., 2017). Similarly, two isomers for coumaroyl *O*- hexoside were detected in peaks **30** and **43** at *m/z* 325.0925 [M-H]-, $C_{15}H_{18}O_8$ (Ibrahim M Abu-Reidah et al., 2013), whereas ferulic acid *O*-hexoside was observed in peak **51** at *m/z* 355.1022 [M-H]-, $C_{16}H_{20}O_9$ (Ibrahim M Abu-Reidah et al., 2013). Ferulic acid was detected in peak **26** as feruloyl *O*- pentosyl hexoside at *m/z* 487.1457 [M-H]-, $C_{21}H_{28}O_{13}$ and fragment at *m/z* 193 corresponding to the loss of a hexoside and pentoside moieties (Ibrahim M Abu-Reidah et al., 2013).

Monomeric proanthocyanidin for (epi)catechin was detected with high abundance in peaks **16** & **28** at *m/z* 289.0716 [M-H]-, $C_{15}H_{14}O_6$ (Ismail et al., 2019). Dimeric procyanidins were seen in peaks **20**, **22** & **45** at *m/z* 577.1346, $C_{30}H_{26}O_{12}$ with fragment at *m/z* 407, and 289 which are characteristic of type B proanthocyanidin previously reported in *A. digitata* fruits (Ismail et al., 2019). Isomers of proanthocyanidin trimers were detected in peaks **23**, **33** & **34** exhibiting molecular ions at *m/z* 865.1992, $C_{45}H_{38}O_{18}$, and distinctive fragment ions at *m/z* 577, 407, 289 (Ismail et al., 2019). Procyanidin tetramer was recognized amply at peak **38** with a molecular ion at *m/z* 1153.2595 [M-H]-, following the same fragmentation pattern as the dimers and trimers (Ismail et al., 2019). All detected proanthocyanidins were grouped in the negative molecular network as group **c** suggestive for their close biosynthetic relationship, except for the tetramer which appeared as a self-looped node.

Interestingly, procyanidins as a major metabolite class in *Adansonia digitata* L. are reported to exert antidiabetic activity *via* various mechanisms of action (Wang, Wang, Ren, & Hu, 2017), including inhibition of α-amylase (Kato, Kushibiki, Inagaki, Kurokawa, & Kawabata, 2017), improvement of insulin resistance (Ogura et al., 2016), reduction of glucogenesis and increase glucose uptake (Li, Sui, Li, Xie, & Sun, 2016).

Flavonols and their glycosides were depicted in peaks **42**, **44**, **46**, **47**, **48**, **49,** & **54**. For example, quercetin-*O*-deoxyhexosyl hexoside isomers were detected in peaks **42** & **44** at *m/z* 609.1457 $[M-H]^-$, $C_{27}H_{30}O_{16}$ showing the loss of a hexoside and deoxyhexoside moieties to reveal quercetin aglycone moiety at *m/z* 301(Ismail et al., 2019). Likewise, kaempferol-*O*-deoxyhexosyl hexoside isomers in peaks **47** & **49** at *m/z* 593.1505 $[M-H]^-$, $C_{27}H_{30}O_{15}$ and fragments at *m/z* 447 and 285 (Ferreres et al., 2017) were identified along with kaempferol-*O*-hexoside isomers in peaks **46** & **54** at *m/z* 447.09314, $C_{21}H_{20}O_{11}$ and fragment ion at *m/z* 285. The identification of kaempferol was confirmed from its peak **48**, observed in the positive ionization mode at *m/z* 287.0543, $C_{15}H_{10}O_6$. Flavonols being antioxidant, anti-inflammatory, are known to suppress the activity of α-amylase, and glucose transporters, and to enhance pancreatic β-cell function (Zamora-Ros et al., 2014).

Furanocoumarins are reported to exhibit numerous biological activities, including anti-inflammatory (J.-K. Lee et al., 2010), vasodilatory (Duarte et al., 1995) and photosensitizing properties (De Leeuw, Assen, Van Der Beek, Bjerring, & Martino Neumann, 2011). They were observed for the first time in peaks **41**, **58** & **59,** as proved from their UV and MS spectra (Ganzera, Sturm, & Stuppner, 1997).

Peak **41** detected in the positive ionization mode exhibited a molecular ion at *m/z* 409.1111 $[M+H]^+$, $C_{19}H_{20}O_{10}$, and a distinct fragment at *m/z* 247 for the loss of a hexoside moiety (Schuster, 1980). Thus, it was ascribed as khellol-*O*-hexoside. While, peaks **58** & **59** showing high abundance, exhibited molecular ions at *m/z* 261.0753 $[M+H]^+$, $C_{14}H_{12}O_5$ and *m/z* 231.0648 $[M+H]^+$, $C_{13}H_{10}O_4$ and were annotated as khellin and visnagin, respectively as concluded from their fragmentation pattern.

Likewise, pyranocoumarins were also detected for the first time in *Adonsonia digitata* fruits. An acylated derivative of the pyranocoumarin, khellactone was recognized at peak **65** as a Na adduct at *m/z* 411.1410 corresponding to $C_{21}H_{24}O_7$ as previously detected by (Olennikov et al., 2019). Its MS_2 spectrum showed fragments at *m/z* 351 $[M+ Na- C_2H_3O_2]^+$ for the cleavage of an acetic acid moiety, *m/z* 245 for the consecutive loss of an isovaleryl moiety (C_5H_8O) followed by *m/z* 227 and 199 for the elimination of H_2O and CO. Consequently it was ascribed as isovaleryl-acetyl khellactone (Olennikov et al., 2019). *O*-substituted esters of khellactone are reported to have numerous biological activities to include antiobesity (Taira et al., 2017), anti-HIV (Xie, Takeuchi, Cosentino, & Lee, 1999) and anti-cancer (J. Y.-C. Wu et al., 2003) activities.

Similarly, peak **66** found in the positive ionization mode, with molecular ion at *m/z* 329.1377, $C_{19}H_{20}O_5$ was annotated as decursin following its fragmentation pattern with fragment ions at *m/z* 245 $[M+H-C_5H_8O]^+$ (H. J. Lee et al., 2009). The antibacterial (S. Lee, Shin, Kim, Oh, & Kang, 2003), anticancer (Ahn, Sim, & Kim, 1995; H. J. Lee et al., 2009) and neuroprotective (Kang & Kim, 2007) properties of decursin have been previously documented.

Fatty acids composition of *Adansonia* fruits compromised saturated fatty acids, monounsaturated fatty acids, and oxygenated fatty acids. Fatty acids were eluted at peaks **67-77** and were annotated based on their molecular formula and fragmentation pattern and in comparison with previously reported literature.

A megastigmane hexoside was observed at peak **55** with a molecular ion at *m/z* 405.2123 $[M-H]^-$ and fragment at *m/z* 225 for the loss of a hexoside moiety and dehydration (K. Singh et al., 2014).

4.1 Conclusion and future perspectives

The current study shows the potential of *Adansonia digitata* L. methanolic fruit pulp crude extract as an antidiabetic plant. The extract has low toxicity both *in vitro* and *in vivo* and a strong antioxidant activity.

The UHPLC/MS showed that the fruit extract contains several chemical groups, such as procyanidins. This chemical class is known to have antidiabetic activity via various mechanisms of action, such as inhibition of α-amylase, improvement of insulin resistance, reduction of glucogenesis, and increase glucose uptake. Moreover, a total of 77 compounds were dereplicated belonging to different classes, including organic acids, sugars, alcohols, phenolics, coumarins, and fatty acids. Almost 50% of the identified metabolites (40 compounds) are reported for the first time in *Adonsonia digitata* fruits.

The biochemical parameters supported the hypothesis of the antidiabetic effect of the *Adansonia digitata* L. However, further, characterization is needed to identify the optimal dose and mode of administration. The histopathological investigation supported the biochemical findings and revealed that the fruit extract has hepatoprotective, and renoprotective effects *in-vivo*.

Further studies are needed for the isolation and investigation of the anti-diabetic effect of the main identified ingredients, such as the procyanidins. Furthermore, a study of the molecular pathway of such active chemicals is necessary to understand the antidiabetic mechanisms better.

References

Abdulfattah, S. Y. (2013). Study of immunological effect of Anastatica hierochuntica (Kaff Maryam) plant Methanolic extract on albino male mice. *Journal of Biotechnology Research Center, 7*(1), 3-10.

Abu-Reidah, I. M., Arráez-Román, D., Al-Nuri, M., Warad, I., & Segura-Carretero, A. (2019). Untargeted metabolite profiling and phytochemical analysis of Micromeria fruticosa L.(Lamiaceae) leaves. *Food Chemistry, 279*, 128-143.

Abu-Reidah, I. M., Arráez-Román, D., Segura-Carretero, A., & Fernández-Gutiérrez, A. (2013). Profiling of phenolic and other polar constituents from hydro-methanolic extract of watermelon (Citrullus lanatus) by means of accurate-mass spectrometry (HPLC–ESI–QTOF–MS). *Food Research International, 51*(1), 354-362.

Adeoye, A. O., & Bewaji, C. O. (2018). Chemopreventive and remediation effect of Adansonia digitata L. Baobab (Bombacaceae) stem bark extracts in mouse model malaria. *Journal of ethnopharmacology, 210*, 31-38.

Agency, F. S. (2002). *McCance and Widdowson's The Composition of Foods Integrated Dataset 2019* (6th ed. ed.): Cambridge, UK: Royal Society of Chemistry.

Ahn, K.-S., Sim, W.-S., & Kim, I.-H. (1995). Detection of anticancer activity from the root of Angelica gigas in vitro. *Journal of Microbiology and Biotechnology, 5*(2), 105-109.

Al-Awar, A., Kupai, K., Veszelka, M., Szucs, G., Attieh, Z., Murlasits, Z., . . . Varga, C. (2016). Experimental Diabetes Mellitus in Different Animal Models. *J Diabetes Res, 2016*, 9051426. doi:10.1155/2016/9051426

Altman, M. F. W. F. D. G. (2002). Guidelines for the Design and Statistical Analysis of Experiments Using Laboratory Animals. *ILAR Journal, 43*(4), 244 - 258.

Amalan, V., Vijayakumar, N., Indumathi, D., & Ramakrishnan, A. (2016). Antidiabetic and antihyperlipidemic activity of p-coumaric acid in diabetic rats, role of pancreatic GLUT 2: In vivo approach. *Biomedicine & Pharmacotherapy, 84*, 230-236.

Amartey, A. A. N., Nsiah, K., & Mensah, F. O. (2015). Plasma levels of uric acid, urea and creatinine in diabetics who visit the Clinical Analysis Laboratory (CAn-Lab) at Kwame Nkrumah University of Science and Technology, Kumasi, Ghana. *Journal of clinical and diagnostic research: JCDR, 9*(2).

Anand, P., Murali, K. Y., Tandon, V., Murthy, P. S., & Chandra, R. (2010). Insulinotropic effect of cinnamaldehyde on transcriptional regulation of pyruvate kinase, phosphoenolpyruvate carboxykinase, and GLUT4 translocation in experimental diabetic rats. *Chemico-Biological Interactions, 186*(1), 72-81. doi:10.1016/j.cbi.2010.03.044

Ananil, K., Hudson, J., & Souzal, C. D. (2000). Investigation of medicinal plants of Togo for antiviral and antimicrobial activities. *Pharmaceutical Biology, 38*(1), 40-45.

Araetus, C. (1856). On causes and symptoms of chronic diseases. In T. b. C. Adam (Ed.). London, (UK): London Sydenham Society.

Bako, H. u. Y., Mohammad, J. a. S., Waziri, P. M., Bulus, T., & Zubairu., M. Y. G. M. M. (2014). Lipid Profile of Alloxan-induced Diabetic Wistar Rats Treated with Methanolic Extract of Adansonia Digitata Fruit Pulp. *Science World Journal, 9*(2).

Barghamdi, B., Ghorat, F., Asadollahi, K., Sayehmiri, K., Peyghambari, R., & Abangah, G. (2016). Therapeutic effects of Citrullus colocynthis fruit in patients with type II diabetes: A clinical

trial study. *Journal of Pharmacy and Bioallied Sciences, 8*(2), 130-134. doi:10.4103/0975-7406.171702

Baum, D. A. (1995). A systematic revision of Adansonia (Bombacaceae). *Annals of the Missouri Botanical Garden, 82*(3), 440-472. doi:10.2307/2399893

Baum, D. A., Small, R. L., & Wendel, J. F. (1998). Biogeography and Floral Evolution of Baobabs (Adansonia , Bombacaceae) as Inferred From Multiple Data Sets. *Syst. Biol., 47*(2), 181-207.

Bell, K. L., Rangan, H., Kull, C. A., & Murphy, D. J. (2015). The history of introduction of the African baobab (Adansonia digitata, Malvaceae: Bombacoideae) in the Indian subcontinent. *Royal Society Open Science, 2*(9). doi:10.1098/rsos.150370

Blois, M. S. (1958). Antioxidant Determinations by the Use of a Stable Free Radical. *Nature, 181*(4617), 1199-1200. doi:DOI 10.1038/1811199a0

Bonnevie-Nielsen, V., Steffes, M., & Lernmark, A. (1981). A major lossin islet mass and B-cell function precedes hyperglycemia in mice given multiple low doses of streptozotocin. *Diabetes, 30*, 424-429.

Braca, A., Sinisgalli, C., De Leo, M., Muscatello, B., Cioni, P. L., Milella, L., . . . Sanogo, R. (2018). Phytochemical profile, antioxidant and antidiabetic activities of Adansonia digitata L.(Baobab) from Mali, as a source of health-promoting compounds. *Molecules, 23*(12), 3104.

Burton-Page, J. (1968). The problem of the introduction of Adansonia digitata into India. *Cambridge University Press, 42*(168), 297-299.

Caluwé, E. D., Halamová, K. i., & Damme, P. V. (2010). Adansonia digitata L. – A review of traditional uses, phytochemistry and pharmacology. *Afrika Focus, 23*(1), 11-51. doi:https://doi.org/10.21825/af.v23i1.5037

Canfield, T. (2010). Propagation of HFF, Human Foreskin Fibroblast Cells. In: Cell Culture SOP.

Cevallos-Cevallos, J. M., Reyes-De-Corcuera, J. I., Etxeberria, E., Danyluk, M. D., & Rodrick, G. E. (2009). Metabolomic analysis in food science: a review. *Trends in Food Science & Technology, 20*(11-12), 557-566. doi:10.1016/j.tifs.2009.07.002

Chadare, F. J., Linnemann, A. R., Hounhouigan, J. D., Nout, M. J. R., & Van Boekel, M. A. J. S. (2008). Baobab Food Products: A Review on their Composition and Nutritional Value. *Critical Reviews in Food Science and Nutrition, 49*(3), 254-274. doi:10.1080/10408390701856330

Chang, W.-C., Wu, J. S.-B., Chen, C.-W., Kuo, P.-L., Chien, H.-M., Wang, Y.-T., & Shen, S.-C. (2015). Protective effect of vanillic acid against hyperinsulinemia, hyperglycemia and hyperlipidemia via alleviating hepatic insulin resistance and inflammation in high-fat diet (HFD)-fed rats. *Nutrients, 7*(12), 9946-9959.

Chao, P. C., Hsu, C. C., & Yin, M. C. (2009). Anti-inflammatory and anti-coagulatory activities of caffeic acid and ellagic acid in cardiac tissue of diabetic mice. *Nutrition & Metabolism, 6*. doi:Artn 3310.1186/1743-7075-6-33

Chiabchalard, M. C. A. (2013). Phytochemical screening and free radical scavenging activities of orange baby carrot and carrot (Daucus carota Linn.) root crude extracts. *Journal of Chemical and Pharmaceutical Research, 5*(4), 97-102.

Clifford, M. N., & Knight, S. (2004). The cinnamoyl–amino acid conjugates of green robusta coffee beans. *Food Chemistry, 87*(3), 457-463.

Colberg, S. R., Sigal, R. J., Yardley, J. E., Riddell, M. C., Dunstan, D. W., Dempsey, P. C., . . . Tate, D. F. (2016). Physical Activity/Exercise and Diabetes: A Position Statement of the

American Diabetes Association. *Diabetes Care, 39*(11), 2065-2079. doi:10.2337/dc16-1728

Contrerasguzman, E. S., & Strong, F. C. (1982). Determination of Tocopherols (Vitamin-E) by Reduction of Cupric Ion. *Journal of the Association of Official Analytical Chemists, 65*(5), 1215-1221.

De Leeuw, J., Assen, Y., Van Der Beek, N., Bjerring, P., & Martino Neumann, H. (2011). Treatment of vitiligo with khellin liposomes, ultraviolet light and blister roof transplantation. *Journal of the European Academy of Dermatology and Venereology, 25*(1), 74-81.

Deen, A. T. A.-., & Al-Naqeb, G. (2014). Hypoglycemic effect and in vitro antioxidant activity of methanolic extract from Argel (Solenostemma Argel) plant. *International Journal of Herbal Medicine, 2*(2), 128-131.

Duarte, J., Pérez-Vizcaíno, F., Torres, A. I., Zarzuelo, A., Jiménez, J., & Tamargo, J. (1995). Vasodilator effects of visnagin in isolated rat vascular smooth muscle. *European journal of pharmacology, 286*(2), 115-122.

Dyck. (2003). *Severity and staging of diabetic polyneuropathy.*

Ebbell, B. (1937). The papyrus Ebers. In. Copenhagen and Oxford: Oxford University Press.

Elflein, J. (2019). Estimated number of diabetics worldwide in 2019 and 2045. Retrieved from https://www.statista.com/statistics/271442/number-of-diabetics-worldwide/

Eromosele, I., Eromosele, C., & Kuzhkuzha, D. (1991). Evaluation of mineral elements and ascorbic acid contents in fruits of some wild plants. *Plant Foods for Human Nutrition, 41*, 151-154.

Farag, M., Mahrous, E., Lübken, T., Porzel, A., & Wessjohann, L. (2013). Classification of commercial cultivars of Humulus lupulus L. (hop) by chemometric pixel analysis of two dimensional nuclear magnetic resonance spectra. *Metabolomics, 10*(1), 21–32. doi:10.1007/s11306-013-0547-4

Farag, M. A., Otify, A., Porzel, A., Michel, C. G., Elsayed, A., & Wessjohann, L. A. (2016). Comparative metabolite profiling and fingerprinting of genus Passiflora leaves using a multiplex approach of UPLC-MS and NMR analyzed by chemometric tools. *Analytical and bioanalytical chemistry, 408*(12), 3125-3143.

Ferreres, F., Magalhães, S., Gil-Izquierdo, A., Valentão, P., Cabrita, A. R., Fonseca, A. J., & Andrade, P. B. (2017). HPLC-DAD-ESI/MSn profiling of phenolic compounds from Lathyrus cicera L. seeds. *Food Chemistry, 214*, 678-685.

Feussner, K., & Feussner, I. (2019). Comprehensive LC-MS-based metabolite fingerprinting approach for plant and fungal-derived samples. In *High-Throughput Metabolomics* (pp. 167-185): Springer.

Fujimatu, E., Ishikawa, T., & Kitajima, J. (2003). Aromatic compound glucosides, alkyl glucoside and glucide from the fruit of anise. *Phytochemistry, 63*(5), 609-616.

Furman, B. L. (2015). Streptozotocin-induced diabetic models in mice and rats. Current protocols in pharmacology. *70*(1), 5-47.

Ganzera, M., Sturm, S., & Stuppner, H. (1997). HPLC-MS and MECC analysis of coumarins. *Chromatographia, 46*(3-4), 197-203.

Garcia, E. J., Oldoni, T. L., Alencar, S. M., Reis, A., Loguercio, A. D., & Grande, R. H. (2012). Antioxidant activity by DPPH assay of potential solutions to be applied on bleached teeth. *Braz Dent J, 23*(1), 22-27. doi:10.1590/s0103-64402012000100004

Gebauer, J., El-Siddig, K., & Ebert, G. (2002). Baobab (Adansonia digitata L.): a Review on a Multipurpose Tree with Promising Future in the Sudan. *Gartenbauwissenschaft, 67*(4), 155-160.

Glaharn, S., Punsawad, C., Ward, S. A., & Viriyavejakul, P. (2018). Exploring pancreatic pathology in Plasmodium falciparum malaria patients. *Scientific reports, 8*(1), 1-8.

Glew, H., Jaget, J. V. d., Lockette, T., Grivetti, E., Smith, C., Pastuszyn, A., & Milsom, M. (1997). Amino acid, fatty acid and mineral composition of 24 indigenous plants of Burkino Faso. *J Food Comp Anal*(10), 205–217.

Gruenwald, J. (2009). Novel botanical ingredients for beverages. *Clin Dermatol, 27*(2), 210-216. doi:10.1016/j.clindermatol.2008.11.003

Gruz, J., Novák, O., & Strnad, M. (2008). Rapid analysis of phenolic acids in beverages by UPLC–MS/MS. *Food Chemistry, 111*(3), 789-794.

Guillarme, D., & Veuthey, J. L. (2017). Theory and Practice of UHPLC and UHPLC–MS. In *Handbook of Advanced Chromatography/Mass Spectrometry Techniques* (pp. 1-38). AOCS Press.

Gupta, P. (2012). Diabetes mellitus and its herbal treatment. *International Journal of Research in Pharmaceutical and Biomedical Sciences, 3*(2).

Gupta, S. C., Patchva, S., & Aggarwal, B. B. (2013). Therapeutic roles of curcumin: lessons learned from clinical trials. *AAPS J, 15*(1), 195-218. doi:10.1208/s12248-012-9432-8

Gwarzo, M. Y., & Bako, H. u. Y. (2013). Hypoglycemic Activity of Methanolic Fruit Pulp Extract of Adansonia digitata on Blood Glucose Levels of Alloxan Induced Diabetic Rats. *International Journal of Animal and Veterinary Advances, 5*(3), 108-113.

Ismail, B. B., Pu, Y., Guo, M., Ma, X., & Liu, D. (2019). LC-MS/QTOF identification of phytochemicals and the effects of solvents on phenolic constituents and antioxidant activity of baobab (Adansonia digitata) fruit pulp. *Food Chemistry, 277*, 279-288.

Jansson, C., Pihlström, T., Österdahl, B. G., & Markides, K. E. (2004). A new multi-residue method for analysis of pesticide residues in fruit and vegetables using liquid chromatography with tandem mass spectrometric detection. *Journal of Chromatography A, 1023*(1), 93-104.

Jin, S., Chang, C., Zhang, L., Liu, Y., Huang, X., & Chen, Z. (2015). Chlorogenic acid improves late diabetes through adiponectin receptor signaling pathways in db/db mice. *PloS one, 10*(4).

Jomard, A., & Osto, E. (2020). High Density Lipoproteins: Metabolism, Function, and Therapeutic Potential. *Frontiers in Cardiovascular Medicine*, 7-39.

Junod, A., Lambert, A. E., Stauffacher, W., & Renold, A. E. (1969). Diabetogenic action of streptozotocin: relationship of dose to metabolic response. *J Clin Invest, 48*(11), 2129-2139. doi:10.1172/JCI106180

Kang, S. Y., & Kim, Y. C. (2007). Neuroprotective coumarins from the root ofAngelica gigas: Structure-activity relationships. *Archives of pharmacal research, 30*(11), 1368-1373.

Kato, E., Kushibiki, N., Inagaki, Y., Kurokawa, M., & Kawabata, J. (2017). Astilbe thunbergii reduces postprandial hyperglycemia in a type 2 diabetes rat model via pancreatic alpha-amylase inhibition by highly condensed procyanidins. *Bioscience, biotechnology, and biochemistry, 81*(9), 1699-1705.

Kerner, W., & Brückel, J. (2014). Definition, Classification and Diagnosis of Diabetes Mellitus. *Experimental and Clinical Endocrinology & Diabetes, 122*(07), 384-386. doi:10.1055/s-0034-1366278

Klein, J., & Alder, L. (2003). Applicability of gradient liquid chromatography with tandem mass spectrometry to the simultaneous screening for about 100 pesticides in crops. *Journal of AOAC International, 86*(5), 1015-1037.

Klopfleisch, R. (2013). Multiparametric and semiquantitative scoring systems for the evaluation of mouse model histopathology-a systematic review. *BMC veterinary research, 9*(1).

Knodell, R. G., Ishak, K. G., Black, W. C., Chen, T. S., Craig, R., Kaplowitz, N., & Wollman, J. (1981). Formulation and application of a numerical scoring system for assessing histological activity in asymptomatic chronic active hepatitis. *Hepatology, 1*(5), 431-435.

Kooti, W., Farokhipour, M., Asadzadeh, Z., Ashtary-Larky, D., & Asadi-Samani, M. (2016). The role of medicinal plants in the treatment of diabetes: a systematic review. *Electron Physician, 8*(1), 1832-1842. doi:10.19082/1832

Ktorza, A., Bernard, C., Parent, V., Penicaud, L., Froguel, P., Lathrop, M., & Gauguier, D. (1997). Are animal models of diabetes relevant to the study of the genetics of non-insulin-dependent diabetes in humans? *Diabetes Metab, 23 Suppl 2*, 38-46.

Kumar, P., Kale, R. K., & Baquer, N. Z. (2012). Antihyperglycemic and protective effects of Trigonella foenum graecum seed powder on biochemical alterations in alloxan diabetic rats. *Eur Rev Med Pharmacol Sci, 16 Suppl 3*, 18-27.

Kumar, S., Singh, R., Vasudeva, N., & Sharma, S. (2012). Acute and chronic animal models for the evaluation of anti-diabetic agents. *Cardiovascular Diabetology, 11*(9).

Ledoux, S. P., & Wilson, G. L. (1984). Effects of streptozotocin on a clonal isolate of rat in-sulinoma cells. *Biochim. Biophys. Acta (BBA), 804*(4), 387–392.

Lee, H. J., Lee, H. J., Lee, E. O., Lee, J. H., Lee, K. S., Kim, K. H., . . . Lü, J. (2009). In vivo anti-cancer activity of Korean Angelica gigas and its major pyranocoumarin decursin. *The American journal of Chinese medicine, 37*(01), 127-142.

Lee, J.-K., Jung, J.-S., Park, S.-H., Park, S.-H., Sim, Y.-B., Kim, S.-M., . . . Suh, H.-W. (2010). Anti-inflammatory effect of visnagin in lipopolysaccharide-stimulated BV-2 microglial cells. *Archives of pharmacal research, 33*(11), 1843-1850.

Lee, M. K., Jeon, H. Y., Lee, K. Y., Kim, S. H., Ma, C. J., Sung, S. H., . . . Kim, Y. C. (2007). Inhibitory constituents of Euscaphis japonica on lipopolysaccharide-induced nitric oxide production in BV2 microglia. *Planta medica, 73*(08), 782-786.

Lee, S., Shin, D.-S., Kim, J. S., Oh, K.-B., & Kang, S. S. (2003). Antibacterial coumarins fromAngelica gigas roots. *Archives of pharmacal research, 26*(6), 449-452.

Li, N. X., Sun, J., H. Shi, H., Yu, L. L., Ridge, C. D., Mazzola, E. P., & Chen, P. (2017). Profiling hydroxycinnamic acid glycosides, iridoid glycosides, and phenylethanoid glycosides in baobab fruit pulp (Adansonia digitata). *Food Research International*(99), 755–761.

Li, X., Sui, Y., Li, S., Xie, B., & Sun, Z. (2016). A-type procyanidins from litchi pericarp ameliorate hyperglycaemia by regulating hepatic and muscle glucose metabolism in streptozotocin (STZ)-induced diabetic mice fed with high fat diet. *Journal of Functional Foods, 27*, 711-722.

Li, X.-N., Sun, J., Shi, H., Yu, L. L., Ridge, C. D., Mazzola, E. P., . . . Chen, P. (2017). Profiling hydroxycinnamic acid glycosides, iridoid glycosides, and phenylethanoid glycosides in baobab fruit pulp (Adansonia digitata). *Food Research International, 99*, 755-761.

Liang, Y., Yan, G. Y., Wu, J. L., Zong, X., Liu, Z., Zhou, H., . . . Li, N. (2018). Qualitative and quantitative analysis of lipo-alkaloids and fatty acids in Aconitum carmichaelii using LC–MS and GC–MS. *Phytochemical Analysis, 29*(4), 398-405.

Lillie, R. D., & Fullmer, H. M. (1976). *Chemical end groups. Histopathologic Technique and Practical Histochemistry*. New York: Mc Graw-Hill.

Lockett, C. T., Calvert, C. C., & Grivetti, L. E. (2000). Energy and micronutrient composition of dietary and medicinal wild plants consumed during drought. Study of rural Fulani, Northeastern Nigeria. *International Journal of Food Sciences and Nutrition, 51*, 195–208.

Lorenz, P., Conrad, J., Bertrams, J., Berger, M., Duckstein, S., Meyer, U., & Stintzing, F. C. (2012). Investigations into the Phenolic Constituents of Dog's Mercury (Mercurialis perennis L.) by LC-MS/MS and GC-MS analyses. *Phytochemical Analysis, 23*(1), 60-71.

Lorenz, P., Conrad, J., Bertrams, J., Berger, M., Duckstein, S., Meyer, U., & Stintzing, F. C. (2012). Investigations into the Phenolic Constituents of Dog's Mercury (Mercurialis perennis L.) by LC-MS/MS and GC-MS analyses. *Phytochemical Analysis, 23*(1), 60-71.

Luka, C. D., & Tijjani, H. (2013). Comparative studies of the aqueous extracts of Ocimum gratissimum, Aloe vera, Brassica oleraceaandIpomoea batatason some biochemical parameters in diabetic rats. *IOSR Journal of Pharmacy and Biological Sciences, 6*(3), 23-29.

Lutter, M., Clark, A. C., Prenzler, P. D., & Scollary, G. R. (2007). Oxidation of caffeic acid in a wine-like medium: Production of dihydroxybenzaldehyde and its subsequent reactions with (+)-catechin. *Food Chemistry, 105*(3), 968-975.

Makila, L., Laaksonen, O., Alanne, A.-L., Kortesniemi, M., Kallio, H., & Yang, B. (2016). Stability of hydroxycinnamic acid derivatives, flavonol glycosides, and anthocyanins in black currant juice. *Journal of agricultural and food chemistry, 64*(22), 4584-4598.

Mamun-or-Rashid, Hossain, S., Hassan, N., Dash, B. K., Sapon, A., & Sen, M. K. (2014). A review on medicinal plants with antidiabetic activity. *Journal of Pharmacognosy and Phytochemistry, 3*(4), 149-159.

Manfredini, S., Vertuani, S., & Buzzoni, V. (2002). Adansonia digitata. II baobab farmacista. *Integr Nutr, 4*(5), 25-29.

Masia, A., Suarez-Varela, M. M., Llopis-Gonzalez, A., & Pico, Y. (2016). Determination of pesticides and veterinary drug residues in food by liquid chromatography-mass spectrometry: A review. *Anal Chim Acta, 936*, 40-61. doi:10.1016/j.aca.2016.07.023

Mohamed A. Farag, Asmaa Otify, Andrea Porzel, Camilia George Michel, Elsayed, A., & Wessjohann, L. A. (2016). "Comparative metabolite profiling and fingerprinting of genus Passiflora leaves using a multiplex approach of UPLC-MS and NMR analyzed by chemometric tools." *Analytical and bioanalytical chemistry, 408*(12), 3125-3143.

Muhammad, I. U., Jarumi, I. K., Alhassan, A. J., Wudil, A. M., & Dangambo, M. A. (2016). Acute toxicity and hypoglycemic activity of aqueous fruit pulp extract of Adansonia digitata L.(Afpead) on alloxan induced diabetic rats. *Journal of Advances in Medical and Pharmaceutical Sciences*, 1-6.

Nam, K.-H., Kim, H. J., Pack, I.-S., Kim, H. J., Chung, Y. S., Kim, S. Y., & Kim, C.-G. (2019). Global metabolite profiling based on GC–MS and LC–MS/MS analyses in ABF3-overexpressing soybean with enhanced drought tolerance. *Applied Biological Chemistry, 62*(1), 15.

Napolitano, A., Cerulli, A., Pizza, C., & Piacente, S. (2018). Multi-class polar lipid profiling in fresh and roasted hazelnut (Corylus avellana cultivar “Tonda di Giffoni”) by LC-ESI/LTQOrbitrap/MS/MSn. *Food Chemistry, 269*, 125-135.

Obizoba, I. C., & Anyika, J. U. (1994). Nutritive value of baobab milk (gubdi) and mixtures of baobab (Adansonia digitata L.) and hungry rice, acha (Digitaria exilis) flours. *Plant Foods for Human Nutrition, 46*, 157-165.

Ogura, K., Ogura, M., Shoji, T., Sato, Y., Tahara, Y., Yamano, G., . . . Tatsuoka, H. (2016). Oral administration of apple procyanidins ameliorates insulin resistance via suppression of pro-inflammatory cytokine expression in liver of diabetic ob/ob mice. *Journal of agricultural and food chemistry, 64*(46), 8857-8865.

Olennikov, D. N., Fedorov, I. A., Kashchenko, N. I., Chirikova, N. K., & Vennos, C. (2019). Khellactone derivatives and other phenolics of Phlojodicarpus sibiricus (Apiaceae): HPLC-DAD-ESI-QQQ-MS/MS and HPLC-UV profile, and antiobesity potential of dihydrosamidin. *Molecules, 24*(12), 2286.

Olmo-García, L., Wendt, K., Kessler, N., Bajoub, A., Fernández-Gutiérrez, A., Baessmann, C., & Carrasco-Pancorbo, A. (2019). Exploring the Capability of LC-MS and GC-MS Multi-Class Methods to Discriminate Virgin Olive Oils from Different Geographical Indications and to Identify Potential Origin Markers. *European journal of lipid science and technology, 121*(3).

Osman, M. A. (2004). Chemical and nutrient analysis of baobab (Adansonia digitata) fruit and seed protein solubility. *Plant foods for human nutrition, 59*(1), 29-33.

Özturk, M. n., Altundag, E., & Gucel, S. (1999). Medicinal and Aromatic Plants (Turkey). *Ethnopharmacology*.

Ozturk, Y., Atlan, V., & Yildizoglu-Ari, N. (1996). Effects of experimental diabetes and insulin on smooth muscle functions. *Pharmacol Rev*(48), 69-112.

Parsa, A. (1959). Medicinal plants and drugs of plant origin in Iran. I. *Plant Food Hum Nutr, 5*, 375-394. doi:10.1007/BF01099755

Perpetuo, G. F., & Salgado, J. M. (2003). Effect of mango (Mangifera indica, L.) ingestion on blood glucose levels of normal and diabetic rats. *Plant Foods for Human Nutrition, 58*, 1–12.

Pettigrew, J. D., Bell, K. L., Bhagwandin, A., Grinan, E., Jillani, N., Meyer, J., . . . Vickers, C. E. (2018). Morphology, ploidy and molecular phylogenetics reveal a new diploid species from Africa in the baobab genus Adansonia (Malvaceae: Bombacoideae). *Systematics and Phylogenys, 61*(6), 1240-1250. doi:10.1002/tax.616006

Pock, J.-M. L., Lumaret, R., Mayne, D., Vall, A. M., Abutaba, Y., Sagna, M., . . . DANTHU, P. (2009). Chloroplast DNA phylogeography suggests a West African centre of origin for the baobab, Adansonia digitata L. (Bombacoideae, Malvaceae). *Molecular Biology, 18*(8), 7. doi:10.1111/j.1365-294X.2009.04144.x

Prevention, C. f. D. C. a. (2020). *National diabetes statistics report*. Retrieved from Online: https://www.cdc.gov/diabetes/pdfs/data/statistics/national-diabetes-statistics-report.pdf

Prism, G. G. S. I., La Jolla, CA, USA. Neurons with action potential frequencies below 0.5 Hz were defined. (Producer).

Qinna, N. A., & Badwan, A. A. (2015). Impact of streptozotocin on altering normal glucose homeostasis during insulin testing in diabetic rats compared to normoglycemic rats. *Drug Des Devel Ther, 9*, 2515-2525. doi:10.2147/DDDT.S79885

Ralaimanerivo, A., Gaydou, E., & Bianchini, J. (1982). Fatty acid composition of seed from six Adansonia species with particular reference to cyclopropane and cydopropene acid. *Lipids*(17), 1-10.

Razafimamonjison, G., Leong Pock Tsy, J. M., Randriamiarinarivo, M., Ramanoelina, P., Rasoarahona, J., Fawbush, F., & Danthu, P. (2017). Fatty acid composition of baobab seed and its relationship with the genus Adansonia taxonomy. *Chemistry & biodiversity, 14*(8), e1600441.

Razanamaro, O., Rasoamanana, E., Rakouth, B., Randriamalala, J. R., Rabakonadrianina, E., Clément-Vidal, A., . . . Danthu, P. (2015). Chemical characterization of floral scents in the six endemic baobab species (Adansonia sp.) of Madagascar. *Biochemical Systematics and Ecology, 60*, 238-248.

Rees, D. A., & Alcolado, J. C. (2005). Animal models of diabetes mellitus. *Diabetic Medicine, 22*, 359-370.

Reichling, J. J., & Kaplan, M. M. (1988). Clinical use of serum enzymes in liver disease. *Digestive diseases and sciences, 33*(12), 1601-1614.

Riss, T. L., Moravec, R. A., Niles, A. L., Duellman, S., Benink, H. A., Worzella, T. J., & Minor, L. (2016). Assay Guidance Manual. In *Cell viability assays*: Eli Lilly & Company and the National Center for Advancing Translational Sciences.

Schuster, R. (1980). Separation and positive identification of compounds in complex sample mixtures using on-line, LC-UV/VIS and LC-MS, direct coupling techniques. *Chromatographia, 13*(7), 379-385.

Selvarani, V., & James, H. (2009). Multiple inflammatory and antiviral activities in Adansonia digitata (Baobab) leaves, fruits and seeds. *Journal of Medicinal Plants Research, 3*(8), 576-582.

Seukep, J. A., Fankam, A. G., Djeussi, D. E., Voukeng, I. K., Tankeo, S. B., Noumdem, J. A., . . . Kuete, V. (2013). Antibacterial activities of the methanol extracts of seven Cameroonian dietary plants against bacteria expressing MDR phenotypes. *Springerplus, 2*(1), 363.

Shahat, A. A. (2006). Procyanidins from Adansonia digitata. *Pharmaceutical Biology*(44), 445–450.

Shigetomi, K., Shoji, K., Mitsuhashi, S., & Ubukata, M. (2010). The antibacterial properties of 6-tuliposide B. Synthesis of 6-tuliposide B analogues and structure–activity relationship. *Phytochemistry, 71*(2-3), 312-324.

Singh, K., Dubey, B. K., Tripathi, A. C., Singh, A. P., & Saraf, S. K. (2014). Natural male contraceptive: phytochemical investigation and anti-spermatogenic activity of Pistia stratiotes Linn. *Natural product research, 28*(16), 1313-1317.

Singh, M. P., & Pathak, K. (2015). Animal models for biological screening of anti-diabetic drugs: An overview. *European Journal of Experimental Biology, 5*(5), 37-48.

Singh, P., Jayaramaiah, R. H., Agawane, S. B., Vannuruswamy, G., Korwar, A. M., Anand, A., . . . Boppana, R. (2016). Potential dual role of eugenol in inhibiting advanced glycation end products in diabetes: proteomic and mechanistic insights. *Scientific reports, 6*(1), 1-13.

Smoot, M. E., Ono, K., Ruscheinski, J., Wang, P. L., & Ideker, T. (2011). Cytoscape 2.8: new features for data integration and network visualization. *Bioinformatics, 27*(3), 431-432.

Sokeng, A. J. T., Sobolev, A. P., Di Lorenzo, A., Xiao, J., Mannina, L., Capitani, D., & Daglia, M. (2019). Metabolite characterization of powdered fruits and leaves from Adansonia digitata L.(Baobab): A multi-methodological approach. *Food Chemistry, 272*, 93-108.

Sokeng, A. J. T., Sobolev, A. P., Lorenzo, A. D., Xiao, J., Mannina, L., Capitani, D., & Daglia, M. (2019). Metabolite characterization of powdered fruits and leaves from Adansonia digitata L.(Baobab): A multi-methodological approach. *Food Chemistry, 272*, 93-108.

Soltesz, G., Patterson, C., & Dahlquist, G. (2007). Worldwide childhood type 1 diabetes incidence – what can we learn from epidemiology? *Pediatric Diabetes, 8*(6), 6–14.

Srinivasan, K. (2006). Fenugreek (Trigonella foenum-graecum): A review of health beneficial physiological effects. *Food Reviews International, 22*(2), 203-224. doi:10.1080/87559120600586315

Srinivasan, K., & Ramarao, P. (2007). Animal models in type 2 diabetes research: An overview. *The Indian Journal of Medical Research*, 451-472.

Srinivasan, K., Viswanad, B., Asrat, L., Kaul, L. C., & Ramarao, P. (2005). Combination of high-fat diet-fed and low-dose streptozotocin-treated rat: a model for type 2 diabetes and pharmacological screening. *Pharmacological research, 52*(4), 313-320.

Steyn, K., & Damasceno, A. (2006). Lifestyle and Related Risk Factors for Chronic Diseases. In D. T. Jamison, R. G. Feachem, M. W. Makgoba, E. R. Bos, F. K. Baingana, K. J. Hofman, & K. O. Rogo (Eds.), *Disease and Mortality in Sub-Saharan Africa. 2nd edition.* NCBI.

Sulaiman, L., Oladele, O., Shittu, I., Emikpe, B., Oladokun, A., & Meseko, C. (2011). In-ovo evaluation of the antiviral activity of methanolic root-bark extract of the African Baobab (Adansonia digitata Lin). *African Journal of Biotechnology, 10*(20), 4256-4258. doi:10.5897/AJB10.2225

Suliman, H. M., Osman, B., Abdoon, I. H., Saad, A. M., & Khalid, H. (2020). Ameliorative activity of Adansonia digitata fruit on high sugar/high fat diet-simulated Metabolic Syndrome model in male Wistar rats. *Biomedicine & Pharmacotherapy, 125*.

Sun, H., Liu, J., Zhang, A., Zhang, Y., Meng, X., Han, Y., & Wang, X. (2016). Characterization of the multiple components of Acanthopanax Senticosus stem by ultra high performance liquid chromatography with quadrupole time-of-flight tandem mass spectrometry. *Journal of separation science, 39*(3), 496-502.

Szkudelski, T. (2001). The Mechanism of Alloxan and Streptozotocin Action in B Cells of the Rat Pancreas. *Physiol. Res.*(50), 536-546.

Taira, N., Nugara, R. N., Inafuku, M., Takara, K., Ogi, T., Ichiba, T., . . . Oku, H. (2017). In vivo and in vitro anti-obesity activities of dihydropyranocoumarins derivatives from Peucedanum japonicum Thunb. *Journal of Functional Foods, 29*, 19-28.

Tohma, H., Gülçin, I., Bursal, E., Gören, A. C., Alwasel, S. H., & Köksal, E. (2017). Antioxidant activity and phenolic compounds of ginger (Zingiber officinale Rosc.) determined by HPLC-MS/MS. *Journal of food measurement and characterization, 11*(2), 556-566.

Tsetegho Sokeng, A. J., Sobolev, A. P., Di Lorenzo, A., Xiao, J., Mannina, L., Capitani, D., & Daglia, M. (2019). Metabolite characterization of powdered fruits and leaves from Adansonia digitata L. (baobab): A multi-methodological approach. *Food Chemistry, 272*, 93-108. doi:10.1016/j.foodchem.2018.08.030

van Meerloo, J., Kaspers, G. J., & Cloos, J. (2011). Cell sensitivity assays: the MTT assay. *Methods Mol Biol, 731*, 237-245. doi:10.1007/978-1-61779-080-5_20

Vanachayangkul, P., Butterweck, V., & Frye, R. F. (2009). Determination of visnagin in rat plasma by liquid chromatography with tandem mass spectrometry and its application to in vivo pharmacokinetic studies. *Journal of Chromatography B, 877*(7), 653-656.

Vertuani, S., Braccioli, E., Buzzoni, V., & Manfredini, S. (2002). Antioxidant capacity of Adansonia digitata fruit pulp and leaves. *Acta Phytotherapeutica, 5*(2), 2-7.

Vertuani, S., Scalambra, E., Molesini, S., Buzzoni, L., Durini, E., Sacchetti, G., & Manfredini, S. (2011). Polyphenols from Adansonia Digitata Extraction, antioxidant analysis and total phenols content.

Wang, F., Wang, J., Ren, M., & Hu, B. (2017). *Effects of pine bark procyanidins extract on blood glucose, blood lipid and antioxidation in diabetic mice.* Paper presented at the 2017 5th International Conference on Machinery, Materials and Computing Technology (ICMMCT 2017).

Weiss, J. F., & Landauer, M. R. (2003). Protection against ionizing radiation by antioxidant nutrients and phytochemicals. *Toxicology, 189*(1-2), 1-20.

Weiss, R. B. (1982). Streptozocin - a Review of Its Pharmacology, Efficacy, and Toxicity. *Cancer Treatment Reports, 66*(3), 427-438.

Wickens, G. E., Goodin, J. R., & Field, D. V. (1985). *Plants for arid lands*: Royal Botanic Gardens, Kew.

Wickens, G. E., & Lowe, P. (2008). *The baobabs: pachycauls of Africa, Madagascar, and Australia.* : Springer.

Wu, J. Y.-C., Fong, W.-F., Zhang, J.-X., Leung, C.-H., Kwong, H.-L., Yang, M.-S., . . . Cheung, H.-Y. (2003). Reversal of multidrug resistance in cancer cells by pyranocoumarins isolated from Radix Peucedani. *European journal of pharmacology, 473*(1), 9-17.

Wu, S., Wilson, A. E., Chang, L., & Tian, L. (2019). Exploring the Phytochemical Landscape of the Early-Diverging Flowering Plant Amborella trichopoda Baill. *Molecules, 24*(21), 3814.

Xie, L., Takeuchi, Y., Cosentino, L. M., & Lee, K.-H. (1999). Anti-AIDS Agents. 37. Synthesis and Structure− Activity Relationships of (3 'R, 4 'R)-(+)-cis-Khellactone Derivatives as Novel Potent Anti-HIV Agents. *Journal of medicinal chemistry, 42*(14), 2662-2672.

Yang, L., Nakamura, N., Hattori, M., Wang, Z., Bligh, S. A., & Xu, L. (2007). High-performance liquid chromatography-diode array detection/electrospray ionization mass spectrometry for the simultaneous analysis of cis-, trans-and dihydro-2-glucosyloxycinnamic acid derivatives from Dendrobium medicinal plants. *Rapid Communications in Mass Spectrometry: An International Journal Devoted to the Rapid Dissemination of Up-to-the-Minute Research in Mass Spectrometry, 21*(12), 1833-1840.

Zamora-Ros, R., Forouhi, N. G., Sharp, S. J., González, C. A., Buijsse, B., Guevara, M., . . . Bredsdorff, L. (2014). Dietary intakes of individual flavanols and flavonols are inversely associated with incident type 2 diabetes in European populations. *The Journal of nutrition, 144*(3), 335-343.

Zekry, S. S. A., Badawy, M. T., Ezzelarab, N., & Abdellatif, A. (2020). Phytotherapy for Diabetes Mellitus; A review of Middle Eastern and North African Folk Medicinal Plants. *Journal of Herbmed Pharmacology*.

Zhang, Y., Yang, L.-J., Jiang, K., Tan, C.-H., Tan, J.-J., Yang, P.-M., & Zhu, D.-Y. (2012). Glycosidic constituents from the roots and rhizomes of Melicope pteleifolia. *Carbohydrate research, 361*, 114-119.

Zhu, R., Liu, H., Liu, C., Wang, L., Ma, R., Chen, B., . . . Zhang, D. (2017). Cinnamaldehyde in diabetes: A review of pharmacology, pharmacokinetics and safety. *Pharmacological research, 122*, 78-89.

Appendix

Table 4: *Histopathological* Scoring of tissue lesions. (Klopfleisch, 2013; Knodell et al., 1981).

Table 3: Score Description

Liver			Kidney		
Lesion	Description	score	Lesion	Description	Score
Degeneration `	Normal	0	Degeneration of tubular epithelium	Normal	0
	< 25% of the entire area	1		< 25% of the entire area	1
	25-50% of the entire area	2		25-50% of the entire area	2
	50-75% of the entire area	3		50-75% of the entire area	3
	>75% of the entire area	4		>75% of the entire area	4
Necrosis	Normal	0	Necrosis of tubular epithelium	Normal	0
	<25% of the area	4		< 25% of the entire area	2
	25-50% of the area	6		25-50% of the entire area	4
	>50% of the area	8		50-75% of the entire area	6
	25-50% of the area + bridging necrosis	10		>75% of the entire area	8
Inflammation	Normal	0	Interstitial infiltration	Normal	0
	<1/3 of the area	1		< 25% of the entire area	1
	1/3 – 2/3 of the area	2		25-50% of the entire area	2
	>2/3 of the area	3		50-75% of the entire area	3
				>75% of the entire area	4

The damage was obtained by summation the entire score of the above histopathological lesions